The value of observed reservoir storage anomalies for improving the simulation of reservoir dynamics in large-scale hydrological models

Seyed-Mohammad Hosseini-Moghari[1], Petra Döll[1, 2]

[1]Institute of Physical Geography, Goethe University Frankfurt, Frankfurt am Main, Germany
[2]Senckenberg Leibniz Biodiversity and Climate Research Centre Frankfurt (SBiK-F), Frankfurt am Main, Germany

Correspondence to: Seyed-Mohammad Hosseini-Moghari (hosseinimoghari@em.uni-frankfurt.de)

Abstract. Human-managed reservoirs alter water flows and storage, impacting the hydrological cycle. Modeling reservoir outflow and storage, which affect water availability for humans and freshwater ecosystems, is challenging because ~~it depends~~they depend on human decisions~~, and there is limited~~. In addition, access to data on reservoir inflows, outflows, storage, and operational rules is very limited. Consequently, large-scale hydrological models either exclude reservoir operations or use calibration-free algorithms ~~for modeling~~to model reservoir dynamics. Nowadays, ~~remotely-sensed information on~~ estimates of reservoir storage anomalies ~~is~~based on remote sensing are a potential resource for calibrating ~~reservoir operation~~the release algorithms for ~~a large number of globally distributed~~many reservoirs worldwide. However, ~~it is not yet clear what~~the impact of calibration against storage anomaly ~~has~~ on simulated reservoir outflow and absolute storage is unclear. In this study, we address this ~~question~~by using in-situ outflow and storage data from 100 reservoirs in the USA (ResOpsUS dataset) to calibrate three reservoir ~~release~~ operation algorithms~~,~~: the well-established Hanasaki algorithm (CH) and two new storage-based algorithms, the Scaling algorithm (SA) and the Weighting algorithm (WA). These algorithms were implemented in the global hydrological model WaterGAP, with their parameters estimated individually for each reservoir and four alternative calibration targets: monthly time series of (1) storage anomaly, (2) estimated storage (calculated based on storage anomaly and GRanD reservoir capacity), (3) storage, and (4) outflow. The first two variables can be obtained from freely available global datasets, while the ~~last~~latter two variables are not publicly ~~available~~accessible for most reservoirs ~~worldwide~~. We found that ~~calibration~~calibrating against outflow ~~does~~did not ~~lead to skillful storage simulations~~result in skillful storage simulations for most of the 100 reservoirs and ~~improves the~~ only slightly improved outflow simulations ~~only slightly more than~~ compared to calibration against the three storage-related ~~calibration~~ targets. Compared to the ~~results of the~~ non-calibrated Hanasaki Algorithm (DH), ~~calibration~~calibrating against both storage anomaly and estimated storage improved the storage simulation ~~and slightly improved~~, whereas the outflow simulation~~.~~ was only slightly improved. Calibration against storage anomaly ~~resulted in 64 (39), 68 (45), and 66 (45)~~ yielded skillful storage simulations for 64 (39), 68 (45), and 66 (45) reservoirs in the case of CH, SA, and WA, respectively, during the calibration (validation) period, ~~as~~ compared to ~~only~~just 16 (15) for DH. ~~Utilizing~~ Using estimated storage instead of storage anomaly does not ~~provide~~offer any added benefit, primarily due to inconsistencies in the observed maximum water storage and storage capacity data from GRanD. ~~Findings show that the~~The default parameters of the Hanasaki algorithm rarely matched the calibrated parameters, highlighting the importance of calibration. Using observed ~~instead of~~ inflow rather than simulated inflow has a ~~more significant effect~~greater impact on improving the outflow simulation than calibration, whereas the opposite is true for the storage simulation. Overall, the performance of the SA and WA algorithms is nearly equal, and both outperform the CH and DH algorithms. Moreover, incorporating downstream water demand into the reservoir

algorithms does not necessarily improve modeling performance due to the high uncertainty in demand estimation. Therefore, to improve the modeling of reservoir storage and outflow in large-scale hydrological models, we recommend calibrating either the SA or the WA reservoir algorithm individually for each reservoir against remote sensing-based storage anomaly, unless in-situ storage data ~~are~~is available, and to improve the reservoir inflow simulation.

1 Introduction

Globally, ~~more than~~over 58,000 large dams (at least 15 meters ~~in height),~~high) capable of impounding 8300 km~~^{3},~~^{3} have been constructed to meet various human needs ~~such as~~, including irrigation, flood control, hydropower generation, domestic water supply, and recreation (Chao et al., 2008; Perera et al., 2021). These dams ~~annually~~ store ~~about~~approximately one-sixth of the annual streamflow in reservoirs (Hanasaki et al., 2006), significantly altering the global freshwater system by increasing evaporation and modifying downstream streamflow (Best, 2019; Tian et al., 2022). About 60% of the seasonal variability in Earth's surface water storage is attributed to human-managed reservoirs, i.e~~.~~., artificial reservoirs and regulated lakes, ~~as~~since the water level of these reservoirs varies on average four times ~~as much as~~more than that of natural lakes (Cooley et al., 2021). Therefore, to accurately depict the hydrologic cycle~~,~~ and assess the ~~inclusion~~impact of reservoir operations on water availability for humans and freshwater ecosystems, including the dynamics of human-managed reservoirs in hydrological models is crucial. ~~This inclusion is supposed to enhance model performance, particularly regarding evapotranspiration and streamflow. At present~~Currently, six out of the 16 global hydrological models contributing to ISIMIP2 (The Inter-Sectoral Impact Model Intercomparison Project, www.isimip.org) simulate the dynamics of human-managed reservoirs (Telteu et al., 2021).

Whereas the outflow from a natural lake strongly depends on the lake's water level ~~of the lake~~ and thus the water storage in the lake, humans ~~control~~manage the outflow from a reservoir. ~~Even though~~Although human decisions ~~on~~regarding the release of water from reservoirs ~~do~~depend, to some ~~degree, depend~~extent, on ~~reservoir~~the reservoir's water storage, they are also ~~influenced~~affected by ~~many~~various other factors, such as downstream water demand, the ~~demand~~need for hydropower production, ~~the need to protect~~flood protection for downstream ~~regions from flooding~~areas, ecosystem ~~requirements~~needs, and legal constraints (Jager and Smith, 2008; Dong et al., 2023). Most reservoirs serve multiple purposes, making their simulation even more complex. However, ~~since reservoir operation~~because the operational (i.e., release) rules of reservoirs and ~~observations of~~observed data on reservoir inflow, outflow, and storage dynamics are rarely publicly ~~accessible~~available, large-scale hydrological models ~~need to~~must resort to calibration-free reservoir operation algorithms that only require information about the reservoir's storage capacity and surface water area. ~~They~~ These algorithms are considered calibration-free ~~algorithms in the sense that~~because they do not require the calibration of reservoir-specific ~~algorithm~~ parameters based on observations of model output variables. ~~These calibration-free~~While these algorithms can ~~only very roughly~~ simulate the decisions of reservoir operators ~~and cannot~~to some extent, they do not account for the unique ~~operation~~operational patterns of each reservoir (Masaki et al., 2018; Turner et al., 2021; Steyaert and Condon, 2024).

All global hydrological models currently ~~use~~employ calibration-free reservoir operation algorithms, which ~~differ regarding~~vary in their formulation and complexity (Telteu et al., 2021). Examples ~~for~~of calibration-free reservoir operation algorithms proposed for large-scale hydrological modeling are described in Dong et al. (2022), Zajac et al. (2017), Haddeland et al. (2006), and Hanasaki et al. (2006) (herein referred to as H06). Dong et al. (2022) and Zajac et al. (2017)

employed different ~~operation~~operational rules for four distinct levels of reservoir storage in their algorithms, whereas Haddeland et al. (2006) developed a prospective optimization algorithm ~~based on~~tailored to the ~~reservoir~~reservoir's purpose. The H06 method is currently implemented in the global hydrological model H08 (Hanasaki et al., 2008) and, in a slightly modified form, in the global hydrological model WaterGAP~~, and~~. It also serves as the ~~foundation~~basis for the Dam-Reservoir Operation model (DROP; Sadki et al., 2023). While studies (e.g., Döll et al., 2009; Vanderkelen et al., 2022) clearly demonstrate that implementing the H06 algorithm leads to improved streamflow simulations compared to ~~not considering~~completely disregarding the reservoir as a surface water body~~ at all~~, there is no consensus (please refer to Döll et al., 2009; Vanderkelen et al., 2022; Gutenson et al., 2020) on whether the H06 algorithm outperforms the natural lake outflow parameterization of Döll et al. (2003) (herein referred to as D03), which assumes that artificial reservoirs behave similarly to natural lakes. It should be noted that ~~simulating~~the simulated reservoir outflow and storage dynamics ~~depends~~depend not only on the reservoir operation algorithm but also on the quality of the simulated inflow, making it ~~difficult~~challenging to assess the adequacy of the algorithm without inflow observations (Vanderkelen et al., 2020).

Several studies have endeavored to fine-tune calibration-free algorithms by adjusting a single parameter for each reservoir, but the results have been unpromising. For example, Gutenson et al. (2020) found that adjusting only one parameter of H06 for 60 non-irrigation reservoirs across the US did not lead to better simulations compared to a calibrated D03. Shin et al. (2019) reported that a new algorithm based on H06, ~~where~~with one parameter~~ was~~ calibrated for 27 reservoirs, could not accurately capture the seasonality in reservoir storage and outflow. ~~Consequently~~As a result, some studies have devised calibration-required algorithms with multiple parameters for each reservoir. Turner et al. (2021) introduced the Inferred Storage Targets and Release Functions (ISTARF) approach, a reservoir operating policy ~~with~~comprising 19 parameters. This approach was applied to 1,930 reservoirs across the ~~US~~U.S. and demonstrated robust improvements in both outflow and storage compared to the H06 model. Although the ISTARF approach is relatively parsimonious in terms of the number of parameters compared to other established calibration-required algorithms — such as those proposed by Yassin et al. (2019) and Turner et al. (2020), which feature 72 (six parameters for each month) and 208 parameters per reservoir (four parameters for each week), respectively — ~~the integration of~~integrating these approaches into large-scale models incurs substantial computational ~~expenses~~costs. More importantly, this approach requires time series data of observed inflow, outflow, and reservoir storage, which can be difficult to obtain outside the US, rendering it infeasible for global-scale modeling. The same limitation applies to some machine learning approaches for simulating reservoir dynamics, such as the artificial neural network approach proposed by Ehsani et al. (2016) and the tree-based reservoir model ~~of~~developed by Chen et al. (2022).

Remotely sensed data on water levels and surface water area of reservoirs are increasingly available~~ and~~. They are being used to derive time series of water storage anomalies or even absolute storage. With recent advancements in spaceborne data, such as the Surface Water and Ocean Topography (SWOT) mission, storage ~~anomalies~~anomaly data can now be gathered even for small reservoirs, providing a valuable source for enhancing resource modeling within large-scale hydrological models (Biancamaria et al., 2016). Examples include HydroSat (Tourian et al., 2022), the Global Reservoir Storage (GRS) dataset (Li et al., 2023), and GloLakes (Hou et al., 2024). This newly available information could be used to calibrate reservoir operation algorithms individually for each reservoir, which is expected to lead to an improved simulation of reservoir dynamics. Remote sensing-derived reservoir storage anomalies were shown to fit reasonably well ~~to~~with in-situ observations, depending on the reservoir and satellite data product~~; storage~~. Storage anomalies, rather than absolute water storage values, should be considered for both~~ the~~ simulated and remote sensing data (Otta et al., 2023). In this regard, Hanazaki et al. (2022) developed a targeted storage-and-release algorithm for global flood modeling, where the release is estimated for four storage zones based on the volume of each zone, flood discharge, and long-term average inflow. They estimated the volume of each storage zone using remote sensing data, while calculating flood discharge ~~was calculated using~~with a probability distribution for 2,169 dams worldwide. The authors reported a 62% improvement in Nash-Sutcliffe Efficiency compared to the version of the CaMa-Flood global hydrodynamic model that did not include the reservoir module. Recently, supported by remote sensing data and a machine learning approach, Shen et al. (2024) developed a satellite-based target storage reservoir operation scheme (SBTS) with seven parameters. This scheme simulates the outflow and storage of flood control reservoirs across four distinct storage zones, ~~using~~utilizing estimated flood storage capacity (FSC) data for 1,178 reservoirs, derived ~~through~~from machine learning~~,~~ trained on reported FSC data from 436 reservoirs. They found that their approach, when using observed inflow, improves reservoir parameterizations, ~~allowing~~enabling the SBTS to generally outperform the methods of Dong et al. (2022), Zajac et al. (2017), and Hanazaki et al. (2022). However, they reported no improvement when the simulated inflow was used. Dong et al. (2023) demonstrated that simultaneous calibrations against reconstructed release and reservoir storage data (using remotely sensed data, model simulations, and in-situ data) considerably improved the performance of reservoir operation algorithms for the Ertan and Jinping I reservoirs in China. However, for global-scale studies, release information is unavailable for most reservoirs. In such cases, calibrating against storage anomaly alone for parameter estimation may degrade outflow simulations due to potential trade-offs between calibrating against different variables (Döll et al., 2024~~,~~; Hasan et al., 2025). The recently published dataset of observed dynamics of US reservoirs, 'ResOpsUS' (Steyaert et al., 2022), which provides time series of daily observed storage, elevation, inflows, and outflows for up to 679 reservoirs across the contiguous US, offers an opportunity to explore this trade-off.

The ~~main~~primary objective of this study is to investigate how monthly time series of observed reservoir-related data can improve the simulation of reservoir outflow and storage in continental or global hydrological models. We focus on the suitability of observed storage ~~anomaly~~anomalies for calibrating reservoir ~~release~~operation algorithms, as these anomalies can be obtained globally through remote sensing-based observations. We compare their informational value to that of scarcer outflow and absolute storage observations, ~~as well as~~along with the simulation results ~~achieved with~~obtained from an uncalibrated reservoir algorithm. We utilized in-situ storage and outflow data from the ResOpsUS dataset for 100 reservoirs in the US to calibrate three reservoir operation algorithms. All algorithms were implemented in the global hydrological model WaterGAP 2.2e (Müller Schmied et al., 2024). The parameters of the algorithms were estimated using ~~as~~the following alternative calibration targets~~,~~: 1) storage anomaly, 2) estimated storage (calculated based on storage anomaly and GRanD reservoir capacity, detailed in section 2.3), 3) storage, and 4) reservoir outflow. Calibration involved optimizing parameters individually for each reservoir, algorithm, and calibration target. ~~To~~Additionally, to explore~~, in addition,~~ the sensitivity of the model results to the quality of the inflow data, we calibrated the algorithms for a subset of 35 reservoirs with available inflow measurements, using observed inflow instead of the inflow simulated by WaterGAP. Finally, for a subset of 21 reservoirs, we ~~determined~~evaluated the ~~effect~~impact of ~~incorporating, in the case of irrigation and water supply reservoirs, the~~including downstream water demand in the ~~reservoir~~ algorithms for irrigation and water supply reservoirs.

2 Methods and Data

2.1 The global hydrological model WaterGAP

WaterGAP simulates the dynamics of water flows and storages on the continents as impacted by human water use and human-managed reservoirs (Müller Schmied et al., 2021). It ~~computes~~calculates sectoral water abstractions~~ as well as~~, along with net abstractions (abstraction minus return flows~~)~~), from surface water bodies (such as reservoirs, lakes, and rivers) and ~~from~~ groundwater. The model has a spatial resolution of 0.5°×0.5° and a daily temporal resolution. However, ~~the~~ model output analysis is ~~normally done at the~~typically conducted on a monthly scale. The current version, 2.2e, has been calibrated in a basin-specific manner against the mean annual streamflow at 1,509 gauging stations worldwide (Müller Schmied et al., 2024). Taking into account the commissioning years, WaterGAP simulates the dynamics of reservoirs with a storage capacity of at least 0.5 km^3, referred to as 'global' reservoirs, using a slightly adapted version of the H06 algorithm (Döll et al., 2009). Smaller reservoirs~~ (termed "local"~~, referred to as 'local' reservoirs~~)~~, are treated as natural lakes (Müller Schmied et al., 2021). A total of 1,255 global reservoirs, with a combined maximum capacity of 5,672 km^3, are integrated into WaterGAP 2.2e, sourced from the GRanD (Lehner et al., 2011) and GeoDAR (Wang et al., 2022) datasets; in addition, 88 regulated lakes are treated like global reservoirs (Müller Schmied et al., 2024). The water balance for a reservoir in WaterGAP is calculated as (Müller Schmied et al., 2021):

$$\frac{dS}{dt} = I + A \cdot \left(P - E_{pot}\right) - GWR - NAs - O \tag{1}$$

where S (m^3) represents reservoir storage, I (m^3/d) denotes inflow into the reservoir from upstream, A (m^2) is the reservoir area, P (m/d) indicates precipitation, E_{pot} (m/d) stands for potential evaporation, GWR (m^3/d) denotes groundwater recharge (only in arid/semiarid regions), NAs (m^3/d) represents potential net abstraction from the reservoir, and O (m^3/d) is the reservoir outflow including release and spill. The surface area A is computed daily as a fraction of the maximum area that depends on the current reservoir storage and its storage capacity. A is reduced by 15 % when S reaches 50% of the reservoir's capacity, and by 75% when S drops to 10% of the capacity (Müller Schmied et al., 2021). Abstraction from a reservoir is permitted only until the water storage level drops to 10% of its total capacity. The implementation of reservoir operation algorithms in WaterGAP is described below. For detailed information on WaterGAP, please refer to Müller Schmied et al. (2021, 2024).

2.2 Reservoir operation algorithms

2.2.1 Hanasaki algorithm as implemented in WaterGAP2.2e

The calibration-free H06 method, in its original formulation, estimates monthly reservoir outflow by distinguishing between irrigation and non-irrigation reservoirs. For non-irrigation reservoirs, this outflow is determined by factors such as the storage at the beginning of the operational year (determined by analyzing the seasonal flow dynamics), the mean annual inflow into the reservoir, and the ~~reservoir~~reservoir's storage capacity. The long-term target for reservoir releases is the mean annual inflow. If reservoir storage at the beginning of an operational year is above normal, releases ~~are increased~~increase throughout the year~~, and~~; conversely, if it is below normal, releases ~~are decreased~~decrease. Therefore, the total release in an operational year depends on the storage level at the start of that year. In the case of irrigation reservoirs, the demand also influences the release (Hanasaki et al., 2006). The H06 algorithm was implemented in WaterGAP on a daily time scale, and the mean annual inflow was adjusted by adding the difference between precipitation and evaporation over the reservoir. This modification aimed to provide a more accurate representation of the reservoir's water balance (Döll et al., 2009).

The first step in the H06 algorithm involves determining the release coefficient for the operational year 'y' (k_y) using the following equation:

$$k_y = \frac{S_{ini}}{a_1 \cdot C} \tag{2}$$

where S_{ini} (km^3) represents the reservoir storage at the start of the operational year; C (km^3) denotes the water storage capacity of the reservoir; and a_1 is a parameter of the H06 method, recommended to be set to 0.85 in its standard form. In the second step, the provisional release is determined. For non-irrigation reservoirs, the provisional release is calculated as follows:

$$R'_d = \overline{I'} \tag{3}$$

in which R'_d (m^3/s) is the provisional release for the day 'd' and $\overline{I'}$ (m^3/s) is the mean annual inflow into the reservoir plus the difference between precipitation and evaporation over the reservoir (for this study, the period 1980-2009). For irrigation reservoirs, the provisional release is computed as follows:

$$R'_d = \begin{cases} a_2 \cdot \overline{I'} \cdot \left[1 + \dfrac{k_{alc} \cdot NAs_d}{\overline{NAs}}\right] & if \;\; \overline{NAs} \; \geq \; a_2 \cdot \overline{I'} \\ \overline{I'} + \; k_{alc} \cdot NAs_d - \; \overline{NAs} & otherwise \end{cases} \tag{4}$$

in which NAs_d (m^3/s) represents the potential net abstraction from surface water bodies for downstream cells of the reservoir for day 'd'; $\overline{NAs}$ (m^3/s) denotes the mean total annual potential net abstraction for downstream cells of the irrigation reservoir; k_{alc} is an allocation coefficient that distributes the abstraction to the upstream reservoirs based on the proportion of $\overline{I'}$ into each reservoir (it equals one if there is only one irrigation reservoir upstream of the demand cells); and a_2 is a parameter specifically for irrigation reservoirs that acts as a partitioner, leading to the use of different equations for reservoirs with a high demand-to-inflow ratio compared to those with a low demand-to-inflow ratio. With a default value of 0.5, this parameter sets the minimum provisional release at 50% of the mean annual inflow during non-crop months. During crop months, the fluctuations in provisional release for reservoirs with a high demand-to-inflow ratio ($\overline{NAs}$ exceeding 50% of mean annual inflow, first equation) correspond to fluctuations in daily net abstraction relative to $\overline{NAs}$. In contrast, reservoirs with a low demand-to-inflow ratio (as per the second equation) align their provisional releases with the daily net abstraction (Hanasaki et al., 2006). The downstream potential net abstraction associated with each reservoir is calculated based on surface water demand for a maximum of five grid cells downstream in the absence of other reservoirs. Otherwise, it extends to the next reservoir. The potential net abstraction information is obtained from the WaterGAP dataset.

With the provisional release determined, the daily release is calculated using the following equation:

$$R_d = \begin{cases} k_y \cdot R'_d & if \;\; c \; \geq \; a_3 \\ \left(\dfrac{c}{a_3}\right)^2 \cdot k_y \cdot R'_d + \left\{1 - \left(\dfrac{c}{a_3}\right)^2\right\} \cdot \; I_d & otherwise \end{cases} \tag{5}$$

where c represents the ratio of C (km^3) to $\overline{I'}$ (km^3/yr); I_d (m^3/s) is the daily inflow into the reservoir for the day 'd'; R_d (m^3/s) is the daily release from the reservoir; and a_3 is a third parameter in the H06 approach, with default value of 0.5. This parameter is also a partitioner that results in the application of different equations for reservoirs with high capacity-to-inflow ratios ($c \geq a_3$) compared to those with low capacity-to-inflow ratios. This implies that for reservoirs with high capacity-to-inflow ratios (first equation), release is independent of daily inflow, while for reservoirs with low capacity-to-inflow ratios (second equation), daily inflow influences the release (Hanasaki et al., 2006). In this study, H06 with default values for a_1, a_2, and a_3 is referred to as the DH algorithm, while H06 with calibrated parameters is referred to as the CH algorithm.

2.2.2 New algorithms

In this study, we introduce and compare two new reservoir operation algorithms that 1) require the reservoir-specific calibration of their parameters; 2) different from H06, utilize daily reservoir water storage as a critical factor in computing daily releases; and (3) do not require water use information to estimate the releases of irrigation reservoirs. Both algorithms include three parameters ~~that are~~ related to different ~~levels of~~ storage levels: above 70% of the reservoir capacity (level 1), between 40% and 70% of the reservoir capacity (level 2), and below 40% of the reservoir capacity (level 3). This classification is based on the observation that the operation rule curve of reservoirs often varies at different storage levels, typically corresponding to different seasons (Dang et al., 2020). Unlike the H06 approach, which employs a single release coefficient for a full year of operation, both new algorithms consider a daily filling ratio, i.e~~.~~., relative water storage ($Srel_d$), as defined by the following equation:

$$Srel_d = \frac{S_d}{C} \tag{6}$$

in which S_d (km^3) is the reservoir storage on day 'd', and C (km^3) indicates the water storage capacity of the reservoir. Both algorithms use $Srel_d$ for release estimation but apply different equations to calculate the release. The following sections describe the release estimation methods employed by these algorithms, i.e., Scaling algorithm (SA) and Weighting algorithm (WA).

2.2.2.1 Scaling algorithm

In the SA algorithm, the daily release at each specific storage level (Level 1, Level 2, or Level 3) is computed as a function of $Srel_d$, mean annual inflow ($\bar{I}$), daily inflow (I_d), the 30-day mean inflow ($\bar{I}_{30d}$), and a parameter associated with that level (Eq. 7). For this purpose, I_d is scaled using the ratio of $\bar{I}$ to $\bar{I}_{30d}$. This ratio represents the general effect of reservoirs in altering the temporal variation of streamflow by storing excess wa ter during high-flow months and releasing it during low-flow months. The multiplication of $\bar{I}$ with $Srel_d$ mimics a prompt response to extreme events where storage can fill up within a few days. The release in the SA algorithm, when water storage is at level n, is calculated as follows:

$$R_d = p_n \cdot \left[Srel_{d-1} \cdot \bar{I} + \frac{\bar{I}}{\bar{I}_{30d}} \cdot I_d \right] \quad \text{for } n = 1, 2, 3 \tag{7}$$

in which $\bar{I}_{30d}$ (m^3/s) represents the mean inflow into the reservoir during the last 30 days. The variable n indicates the storage level at time *d-1*, and p_n is the parameter assigned to storage level *n* (one parameter assigned to each storage level). Levels 1, 2, and 3 correspond to $Srel$ as follows: Level 1 for above 0.7, Level 2 for between 0.4 and 0.7, and Level 3 for below 0.4. (see Fig. 1). The ~~parameters value~~parameter values need to be determined through the calibration process. These parameters enable us to adjust the mean release, while temporal variability is estimated inside the square brackets.

2.2.2.2 Weighting algorithm

The WA ~~are~~is the same as SA method in most ~~part~~parts of the release calculation~~,~~; however, in contrast to the SA method, WA does not consider I_d to compute the release and solely relies on $Srel_d$ for weighting $\bar{I}$ and $\bar{I}_{30d}$. Therefore, the contribution of long-term inflow is higher at higher storage levels, while its contribution decreases ~~with lower~~as storage levels decrease. Conversely, the contribution of inflow from the last 30 days increases as storage decreases. A maximum of 30% of $\bar{I}_{30d}$ contributes to release estimation at higher storage levels ($Srel \geq 0.7$), while it reaches 100% when the reservoir is empty, which is identical to run-of-the-river flow. In the WA algorithm, when water storage is at level *n*, the release is estimated as follows:

$$R_d = q_n \cdot [Srel_{d-1} \cdot \bar{I} + (1 - Srel_{d-1}) \cdot \bar{I}_{30d}] \qquad \text{for } n = 1, 2, 3 \tag{8}$$

where q_n is the parameter assigned to storage level *n* that needs to be determined (see Fig. 1). We opted for $\bar{I}_{30d}$ over I_d assuming that release decisions may rather be based on the past inflow over a ~~longer~~more extended period and not on the inflow on just the previous day.

Contrary to the H06 approach, where the release is independent of inflow in reservoirs with large storage capacity relative to the annual inflow (~~meaning~~resulting in a constant release throughout the year, see Eq. 5), both new algorithms consider the impact of inflow on release in all reservoirs. This impact varies with different seasons and storage levels, leading to variability in release throughout the year, which is more realistic (see Eq. 7 and Eq. 8). It should be noted that the new algorithms do not distinguish between irrigation and non-irrigation reservoirs; therefore, no water use data is required for their application, making their implementation easier than the H06 algorithm. This is because ~~the estimation of~~estimating downstream water demand ~~at~~on a large scale is ~~generally~~usually very uncertain, and reservoirs are ~~usually~~typically designed for multiple purposes.

In each of the three algorithms, if S_d falls below 10 percent of the storage capacity (C), the calculated R_d is adjusted to $0.1 \cdot R_d$ if the available water is sufficient; otherwise, the entire S_d will be released. Finally, the reservoir outflow is calculated as follows:

$$O_d = R_d + SP_d \tag{9}$$

where O_d (m^3/s) and SP_d (m^3/s) are the reservoir outflow and the spill from the reservoir during day 'd', respectively. SP_d is calculated as the difference between S_d and C, where S_d exceeds C; otherwise, it is zero.

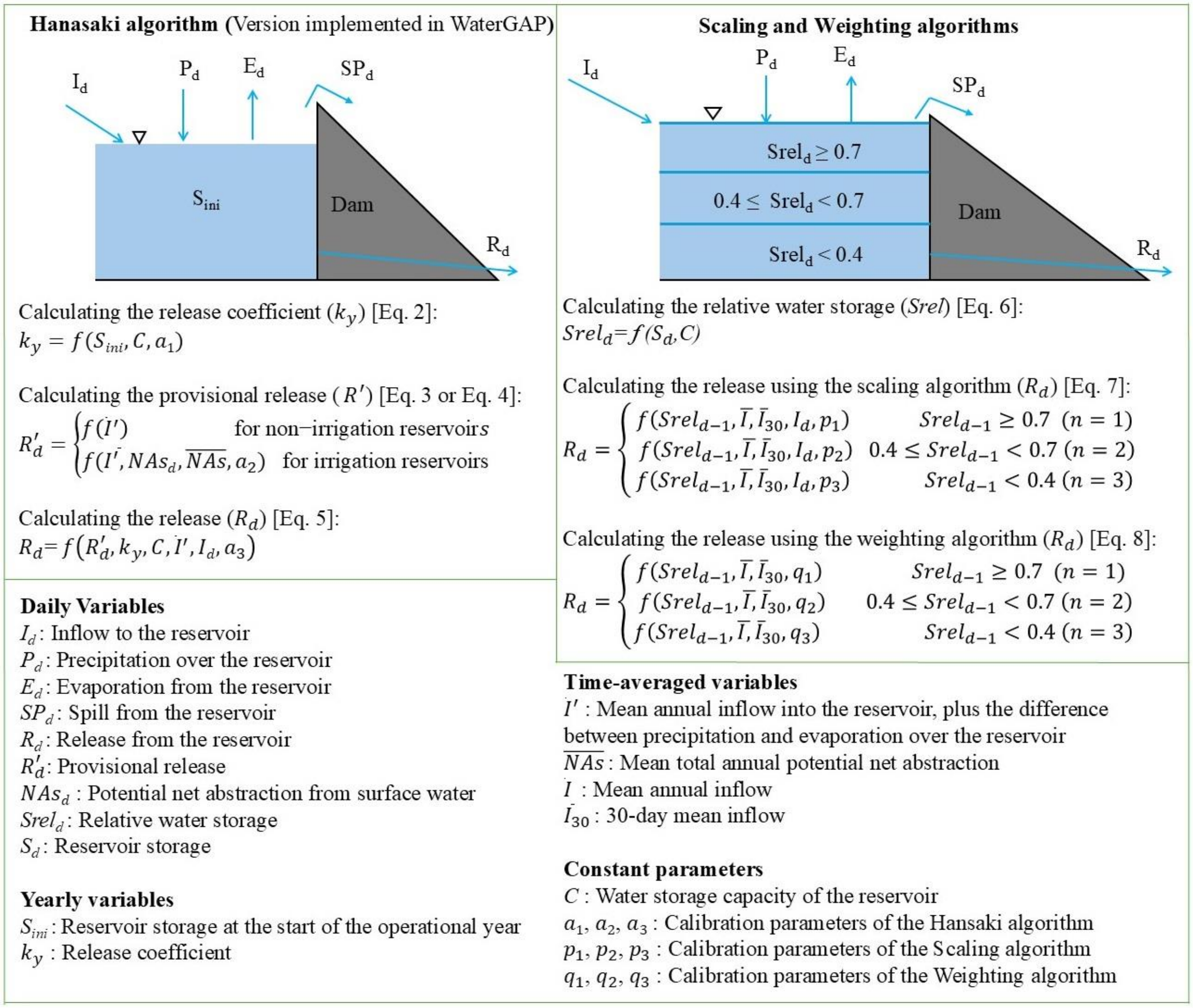

Calculating the release coefficient (k_y) [Eq. 2]:
$k_y = f(S_{ini}, C, a_1)$

Calculating the provisional release (R') [Eq. 3 or Eq. 4]:

$$R'_d = \begin{cases} f(\bar{I}') & \text{for non−irrigation reservoirs} \\ f(\bar{I}', NAs_d, \overline{NAs}, a_2) & \text{for irrigation reservoirs} \end{cases}$$

Calculating the release (R_d) [Eq. 5]:
$R_d = f\left(R'_d, k_y, C, \bar{I}', I_d, a_3\right)$

Daily Variables
I_d: Inflow to the reservoir
P_d: Precipitation over the reservoir
E_d: Evaporation from the reservoir
SP_d: Spill from the reservoir
R_d: Release from the reservoir
R'_d: Provisional release
NAs_d : Potential net abstraction from surface water
$Srel_d$: Relative water storage
S_d: Reservoir storage

Yearly variables
S_{ini}: Reservoir storage at the start of the operational year
k_y : Release coefficient

Calculating the relative water storage (*Srel*) [Eq. 6]:
$Srel_d = f(S_d, C)$

Calculating the release using the scaling algorithm (R_d) [Eq. 7]:

$$R_d = \begin{cases} f(Srel_{d-1}, \bar{I}, \bar{I}_{30}, I_d, p_1) & Srel_{d-1} \geq 0.7 \ (n = 1) \\ f(Srel_{d-1}, \bar{I}, \bar{I}_{30}, I_d, p_2) & 0.4 \leq Srel_{d-1} < 0.7 \ (n = 2) \\ f(Srel_{d-1}, \bar{I}, \bar{I}_{30}, I_d, p_3) & Srel_{d-1} < 0.4 \ (n = 3) \end{cases}$$

Calculating the release using the weighting algorithm (R_d) [Eq. 8]:

$$R_d = \begin{cases} f(Srel_{d-1}, \bar{I}, \bar{I}_{30}, q_1) & Srel_{d-1} \geq 0.7 \ (n = 1) \\ f(Srel_{d-1}, \bar{I}, \bar{I}_{30}, q_2) & 0.4 \leq Srel_{d-1} < 0.7 \ (n = 2) \\ f(Srel_{d-1}, \bar{I}, \bar{I}_{30}, q_3) & Srel_{d-1} < 0.4 \ (n = 3) \end{cases}$$

Time-averaged variables
$\bar{I}'$: Mean annual inflow into the reservoir, plus the difference between precipitation and evaporation over the reservoir
$\overline{NAs}$: Mean total annual potential net abstraction
$\bar{I}$: Mean annual inflow
$\bar{I}_{30}$: 30-day mean inflow

Constant parameters
C : Water storage capacity of the reservoir
a_1, a_2, a_3 : Calibration parameters of the Hansaki algorithm
p_1, p_2, p_3 : Calibration parameters of the Scaling algorithm
q_1, q_2, q_3 : Calibration parameters of the Weighting algorithm

Figure 1. Overview of the process to calculate reservoir release using the Hanasaki (H06), Scaling (SA) and Weighting (WA) algorithms, indicating the required inputs as well as the equation numbers where the complete equations can be found in the text. The left panel details the H06 algorithm implemented in WaterGAP, ~~with~~outlining the steps for calculating the release coefficient, provisional release, and release. The H06 algorithm requires reservoir capacity, storage values at the start of the operational year, daily inflow, precipitation, evaporation data, and daily potential net abstraction data for irrigation reservoirs. The right panel presents SA and WA, indicating the calculation of relative water storage and the release computation as a function of three reservoir water storage levels (n = 1, 2, or 3). SA and WA ~~release~~releases are calculated based on reservoir capacity, daily storage, precipitation, evaporation, and inflow. The time-averaged variables are derived from daily data. For the H06 algorithm DH, the default values for *a₁*, *a₂*, and *a₃* are 0.85, 0.5, and 0.5, respectively.

2.3 Data

The ResOpsUS dataset (Steyaert et al., 2022), which ~~served for calibrating~~was used to calibrate and ~~evaluating~~evaluate the three algorithms in this study, encompasses daily in-situ records of inflow, storage, outflow, elevation, and evaporation for up to 679 US reservoirs. The available data ~~spans~~covers the years from 1930 to 2020, determined by ~~each dam's~~the commissioning year of each dam and ~~data~~the availability of data. In this study, data on reservoir inflow (daily), outflow (monthly), and storage (monthly) from 1980 to 2019 were considered, divided into two distinct periods: a calibration phase spanning from 1980 to 2009, and a validation phase covering the years 2010 to 2019. Monthly data were computed from daily records, excluding months with more than one week of missing values. Subsequently, we applied filters to the dataset, considering only reservoirs with a minimum data length of five years~~,~~ and a minimum reservoir capacity of 0.5 ~~km^3, as well~~

~~as ensuring~~km^3. Additionally, we ensured that there is only one reservoir per 0.5~~°×~~ ° × 0.5 ° grid cell and that no negative values are present. This resulted in 100 reservoirs, with 35 having data for storage, inflow, and outflow, and 65 having data for storage and outflow only. The minimum number of monthly data values for the 65 (35) reservoirs was 111 (252) for the calibration period and 65 (59) for the validation period. The ~~reservoirs'~~reservoir storage capacities (C) range from 0.5 km^3 to 36.7 km^3 based on the GRanD dataset (Lehner et al., 2011). Out of the total 100 reservoirs, nine are irrigation reservoirs. Detailed information on each reservoir is provided in Table S1.

Using in-situ storage data, we derived two additional storage-related variables: the time series of storage anomaly and estimated storage. These variables can also be estimated using remote sensing data. ~~Storage~~The storage anomaly time series for each reservoir is calculated by subtracting the mean storage during the calibration period from the in-situ storage data for each reservoir. However, the storage anomaly lacks information about the bias term, and calibrating against it can ~~result in~~lead to a simulated storage time series that significantly deviates from the observed water storage. Having actual absolute storage is ~~advantageous~~beneficial, as reservoirs are the only surface water bodies for which we can model absolute storage within ~~the~~ WaterGAP. To provide an alternative, we calculated the "estimated storage time series"; this term refers to storage values that are not observed directly but are estimated using storage anomaly and the reservoir capacity C. First, we determined the storage ~~changes~~change time series by subtracting the initial month's storage anomaly value from the monthly storage anomaly values. Assuming the reservoir reaches maximum capacity at least once between 1980 and 2009, we calculated the maximum monthly storage change, ~~termed~~referred to as Dif_{max}. We then subtracted Dif_{max} from the GRanD reservoir storage capacity to estimate the initial water storage for the first month. The estimated storage time series is then obtained by adding the storage changes to this estimated initial water storage. Since the data are monthly, and daily maximum storage is generally higher, we applied a 1.2 scaling factor to Dif_{max}. This adjustment means that Dif_{max} used in our calculations is 20% higher than the initially calculated value. This 20% increase is derived from the mean difference between the maximum daily storage and the monthly storage observed in 100 studied reservoirs (see Table S1). The calculation of estimated storage can be performed using either absolute storage or storage anomaly, as the time series of storage changes would remain the same in both cases. An example using GRanD ID 597 (Glen Canyon Dam, Lake Powell) clarifies the calculation of storage anomaly and estimated storage. The mean observed storage value between 1980 and 2009 for Glen Canyon Dam is 22.45 km^3. To obtain the storage anomaly time series for this reservoir, the value of 22.45 km^3 is subtracted from all storage data for the reservoir over the entire period (1980–2019). For calculating estimated storage, the Dif_{max} is 6.6 km^3, which occurred in July 1983 (see Fig. S1). This is calculated as the storage anomaly value in July 1983 minus the initial storage anomaly value in January 1980. The initial storage is estimated as 25.1 km^3 (the reservoir capacity reported by GRanD) minus 7.9 km^3 (6.6 km^3×1.2). This gives an initial storage value of approximately 17.2 km^3. Storage changes are then added to the estimated initial storage to obtain the time series of estimated storage (Fig. S1c), e.g., the estimated storage for July 1983 is 23.8 km^3, which is the sum of 17.2 km^3 and 6.6 km^3.

2.4 Model variants and calibration approach

The three reservoir operation algorithms were implemented in WaterGAP. For each algorithm, the algorithm-specific parameters (a_1, a_2, and a_3 for the CH, p_1, p_2, and p_3 for the SA and q_1, q_2, and q_3 for the WA) were estimated by optimizing the Kling–Gupta Efficiency (KGE) (Kling et al., 2012), including the trend term (see Eq. 10). This optimization was performed through a single-objective calibration against the monthly time series of four variables: outflow, storage, storage anomaly, and estimated storage (see Section 2.3). The parameters of each algorithm were calibrated using a grid search approach. Reservoir outflow and storage time series were simulated for all parameter sets listed in Table S2, and the parameter set corresponding to the highest KGE was selected. The parameter estimation using storage anomaly and estimated storage serves as the main experiment, as the primary emphasis of this study is on exploring the added value of incorporating storage anomaly (which facilitate the calibration of reservoir algorithms using remote sensing data in regions where in-situ storage time series are unavailable) into the calibration of reservoir operation algorithms.

As in previous studies by Dong et al. (2023), Turner et al. (2021), and Shin et al. (2019), the uncalibrated H06 (DH) is used as a benchmark. For comparison purposes, in all calibration experiments based on WaterGAP inflow, the inflow into reservoirs simulated by the DH algorithm was used to ensure that the same inflow data were applied across all algorithms. To achieve this, WaterGAP was first run with the DH algorithm to save the reservoir inflow data. These inflow data were then read from the saved files and used as the inflow source to model each reservoir independently. As a result, the inflow into all reservoirs, regardless of their position, was based on the DH algorithm when applying the CH, SA, and WA algorithms, meaning that the operations of upstream reservoirs did not affect those of downstream reservoirs. The calibration runs were initialized by running WaterGAP five times for the year 1979~~ to allow~~, allowing water storages to reach a relatively stable equilibrium state.

In addition to the inflow simulated by WaterGAP, we also assessed the algorithms based on observed inflow where available. This was done to ~~check~~evaluate the performance of reservoir operation algorithms in the presence of high-quality inflow data, as poor inflow data can significantly impact the performance of ~~the~~these algorithms~~ may be heavily impacted by poor inflow data~~ (Vanderkelen et al., 2022). Moreover, we assessed the impact of distinguishing irrigation and supply reservoirs from other reservoirs. The distinction for irrigation reservoirs is the default approach for the H06 algorithm; however, here we also applied this distinction for supply reservoirs, as ~~also ~~their outflow also depends on downstream demand. To this end, we modeled 21 reservoirs (nine irrigation and 12 supply reservoirs) in two different ways for all algorithms: one ~~including~~that included downstream demand and the other ~~without considering~~that did not consider it. The purpose of this comparison is to evaluate whether including downstream demand, despite the high uncertainty in water demand estimation for the reservoirs, enhances the outflow and storage simulation~~,~~ or whether it ~~may not add~~adds value ~~and instead introduce~~without introducing unnecessary complexity. In the case of the SA and WA approaches for considering downstream demand, the process involves using the provisional release R'_d instead of $\overline{I}$ in Eqs. 7 and 8. Therefore, similar to the DH algorithm, Eq. 4 was used with the default value for the parameter a_2~~. However, instead of using $\overline{I'}$,~~ to estimate R'_d. Please note that, since the WA and SA approaches work with $\overline{I}$ ~~-~~and not $\overline{I'}$, $\overline{I}$ was applied in Eq. 4~~. The resulting R'_d from Eq. 4 then replaced~~ instead of $\overline{I'}$ in the SA and WA approaches.$\overline{I}$~~ in Eqs. 7 and 8 for estimating R_d.~~

Table 1 shows a summary of the different calibration variants. In Table 1, each calibration variant is characterized by a combination of a reservoir operation algorithm, a calibration variable, an inflow source, and whether ~~or not ~~downstream demand is considered or not. For example, calibrating the CH algorithm against outflow using inflow simulated by WaterGAP while considering downstream water demand represents one calibration variant. Thus, each reservoir operation algorithm comprises 12 calibration variants (eight utilizing WaterGAP inflow and four using observed inflow), leading to a total of 36 calibration variants.

Table 1. Components of the different calibration variants, comprising 36 variants in total, with 12 variants for each algorithm. Each algorithm includes four variants ~~using~~that use WaterGAP inflow with downstream demand considerations

(calibrated against outflow, storage, storage anomaly, and estimated storage), four variants ~~using~~that use WaterGAP inflow without downstream demand, and four variants ~~using~~that use observed inflow. Each calibration variant is defined by the combination of a reservoir operation algorithm, calibration variable, inflow source, and the consideration or non-consideration of downstream demand. For CH, the default approach incorporates the downstream demand of irrigation reservoirs, while the opposite is true for SA and WA. Additionally, considering the downstream demand for supply reservoirs is not the default approach for any of the reservoir operation algorithms. For calibration variants that utilize observed inflow, only the default approach of each algorithm is considered.

Operation algorithm	Calibration variable	Inflow source	Downstream demand considered?
CH	Outflow Storage Storage anomaly Estimated storage	WaterGAP	Yes[1]
			No
		Observation	Yes[2]
SA WA	Outflow Storage Storage anomaly Estimated storage	WaterGAP	Yes[1]
			No
		Observation	No

[1] Water demand is considered for irrigation and supply reservoirs, i.e., 21 out of 100 studied reservoirs.

[2] Water demand is considered for irrigation reservoirs, i.e., two out of 35 studied reservoirs with observed inflow.

2.5 Performance evaluation metrics

The performance of the reservoir operation algorithms was evaluated using KGE and the normalized root mean square error (nRMSE). KGE is widely used for model calibration and evaluation, as it simultaneously considers multiple important aspects of model performance, providing a comprehensive assessment (Beck et al., 2019; Lamontagne et al., 2020). The use of nRMSE offers additional insights by focusing on the magnitude of errors. Following Hosseini-Moghari et al. (2020), we incorporated the trend component into the conventional KGE equation as follows:

$$KGE = 1 - \sqrt{(R_{KGE} - 1)^2 + (\,B_{KGE} - 1)^2 + (V_{KGE} - 1)^2 + (T_{KGE} - 1)^2} \quad (10)$$

$$R_{KGE} = \frac{cov(sim, obs)}{\sigma_{sim} \cdot \sigma_{obs}} \quad (11)$$

$$B_{KGE} = \frac{\overline{sim}}{\overline{obs}} \quad (12)$$

$$V_{KGE} = \frac{\sigma_{sim}/\overline{sim}}{\sigma_{obs}/\overline{obs}} \quad (13)$$

$$T_{KGE} = \frac{T_{sim}}{T_{obs}} \quad (14)$$

where R_{KGE} represents the correlation coefficient between observed (*obs*) and simulated (*sim*) time series; B_{KGE} denotes the bias of the mean simulated ($\overline{sim}$) compared to the mean of observed ($\overline{obs}$), V_{KGE} is the variability component that denotes the ratio of the standard deviation of the simulated (σ_{sim}) to the standard deviation of the observed (σ_{obs}) time series, divided by their mean, and T_{KGE} represents the ratio of the linear trend of the simulated time series (T_{sim}) to the observed one (T_{obs}). In the case of calibrating against storage anomaly, we did not divide σ by the mean, as the mean for storage anomaly is zero. Similarly, the B_{KGE} component was not considered in calculating KGE related to storage anomaly. The optimal value for the KGE and its four components is 1. The KGE range is $(-\infty, 1]$, while R_{KGE} ranges from -1 to 1; B_{KGE}, V_{KGE} and T_{KGE} can vary between $-\infty$ and $+\infty$. Following Knoben et al. (2019), a KGE value above -0.73 indicates that the model performs better than the mean of observations if the trend component is included in the KGE.

The normalized root mean square error (nRMSE) is calculated as:

$$nRMSE = \frac{\sqrt{\frac{1}{T}\sum_{t=1}^{T}(obs_t - sim_t)^2}}{\sigma_{obs}} \tag{15}$$

The perfect value for nRMSE is zero. Normalizing the RMSE with the standard deviation of observations brings this metric closer to the Nash-Sutcliffe Efficiency (NSE), but different from the NSE, the nRMSE cannot become negative (Turner et al., 2021).

3 Results

3.1 Performance of calibration variants in the case of simulated inflow into reservoirs

We found that calibrating against observed water storage, water storage anomaly, or estimated water storage (derived from storage anomaly and GRanD ~~storage~~ capacity) improves the very poor simulation of storage by the calibration-free algorithm (DH) ~~for~~during both ~~the~~ calibration and validation ~~periods in the case of~~ for all three algorithms (Table 2). In the case of DH, storage simulation is skillful, i.e. with a $KGE_{storage} > -0.73$~~,~~ for only 16% of the 100 reservoirs ~~during~~in the calibration period~~,~~ and ~~for~~ 15% ~~during~~in the validation period. Calibration of the H06 reservoir operation algorithm (CH) achieves skillful storage simulations for 64% (39%) of the reservoirs when calibrated against storage anomaly and for 69% (32%) of the reservoirs when calibrated against estimated storage during the calibration (validation) period. Both SA and WA ~~outperform~~perform better than CH in storage simulation when calibrated against storage-related variables for ~~both~~ the calibration and validation ~~period~~periods (Table 2 and Fig. 2). However, the fit of simulated to observed storage remains poor during the validation period, ~~in particular~~particularly after calibration against the storage anomaly and estimated storage (Table 2 and Fig. 2).

Table 2. The number of reservoirs out of 100 in which KGE values are greater than the benchmark thresholds of -0.73 during the calibration (validation) phase. All algorithms were calibrated against outflow, storage, storage anomaly, ~~as well as~~and estimated storage, using KGE as the objective function. The inflow data is sourced from the WaterGAP model.

Calibrated variable	Algorithm	KGE > -0.73	
		Outflow	Storage
—	DH	63 (56)	16 (15)
Outflow	CH	78 (68)	22 (30)
	SA	86 (71)	14 (24)
	WA	86 (69)	20 (30)
Storage	CH	68 (69)	91 (46)
	SA	66 (67)	98 (68)
	WA	67 (66)	100 (55)
Storage anomaly	CH	67 (69)	64 (39)
	SA	67 (69)	68 (45)
	WA	71 (70)	66 (45)
Estimated storage	CH	70 (69)	69 (32)
	SA	65 (68)	69 (46)
	WA	67 (70)	74 (41)

~~Calibration against~~Calibrating for storage-related variables only slightly improves the mostly poor simulations of reservoir outflow during the calibration period~~ and shows a bit more improvement~~, with slightly better outcomes observed in the validation period (Table 2 and Fig. 2). Skillful outflow simulations were achieved for 86% of the reservoirs when either SA or WA were calibrated against outflow, compared to 78% for CH and 63% for DH during the calibration phase. However, skillful storage simulations were observed in only 14% (24%) and 20% (30%) of the reservoirs for SA and WA, respectively, compared to 22% (30%) for CH and 16% (15%) for DH in the calibration (validation) phase (Table 2). The performances of outflow simulations with CH, SA, and WA are very similar ~~in~~during both the calibration and validation periods, except ~~in the case of calibration~~when calibrating against observed outflow ~~for~~in the calibration period. In this case, SA and WA achieved positive KGE$_{outflow}$, with medians of 0.15 for SA and ~~of~~ 0.13 for WA. Calibrating ~~against~~with respect to outflow improves the correlation, variability, and trend of the simulated outflow ~~compared~~relative to DH ~~for~~across all three algorithms, while the bias ~~is not affected much~~remains largely unchanged (Figs. S2-S5). On average, outflow trends are underestimated. Calibrating against outflow worsens both the correlation and variability of storage simulations across all three algorithms during the calibration phase, though it notably improves the bias component (Figs. S2-S4). Model performance ~~regarding~~related to storage is not affected in a relevant manner by calibration against outflow and remains very poor. When algorithms are calibrated against outflow, the mean observed storage ~~generally remains~~is usually a better estimator than the simulated storage.

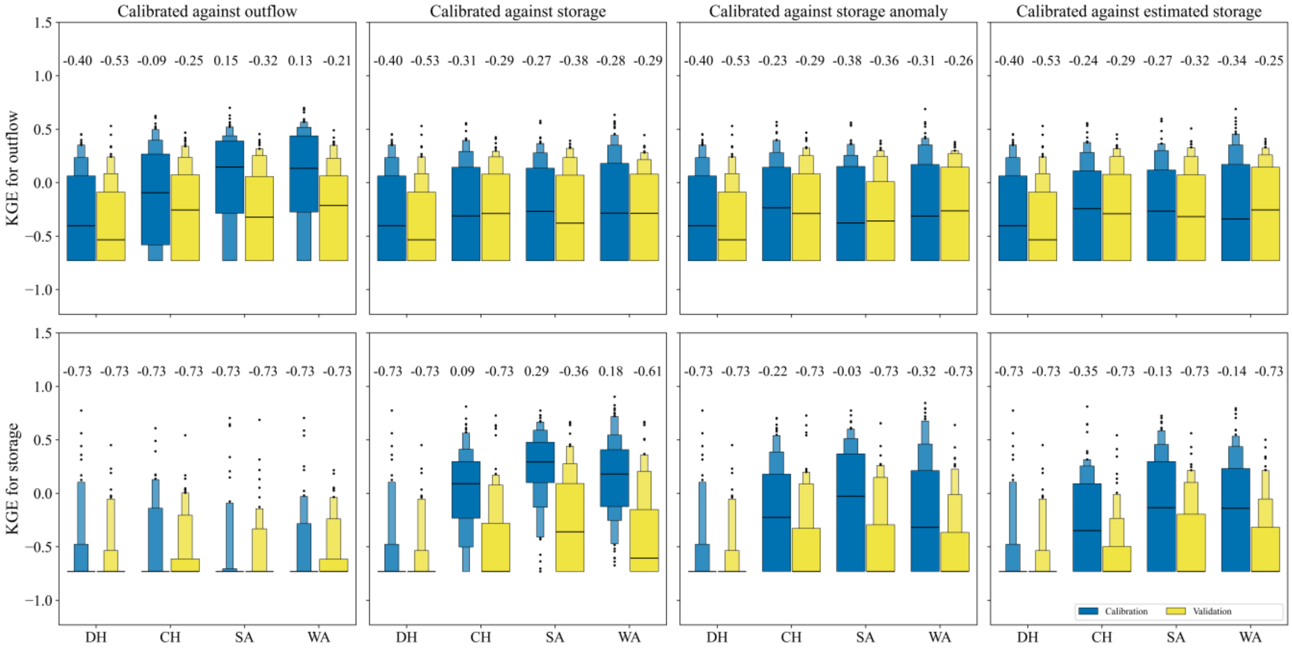

Figure 2. Letter-value plots of KGE for outflow and storage of 100 studied reservoirs for DH, CH, SA, and WA algorithms for the calibration period (1980-2009, in blue) and validation period (2010-2019, in yellow). All algorithms are calibrated against outflow (first column), storage (second column), storage anomaly (third column), ~~as well as~~and estimated storage (fourth column~~)~~), using KGE as the objective function. The values at the top of the panels are the median KGE (indicated by the horizontal line). KGE values below the benchmark threshold of -0.73 are set to -0.73. The widest box contains 50% of the 100 data points, the second widest 25% of the data (12.5% in the upper box and 12.5% in the lower box), the third widest 12.5%, and so on. The inflow data is sourced from the WaterGAP model.

Calibrating against storage (Fig. 2, second column~~ of Fig. 2) leads to~~) yields the highest KGE$_{storage}$ values~~;~~, with a median ~~KGE$_{storage}$~~ of 0.29, SA outperforms CH and WA, while ~~the~~ KGE$_{outflow}$ and its component values ~~for~~across the three algorithms are similar (Figs. S2-S5). ~~Calibrating~~Calibration against storage anomaly (third column in Fig. 2) or estimated storage (fourth column in Fig. 2) improves both storage and outflow simulations ~~as~~ compared to DH, but the fit to observed storage is ~~considerably~~ worse than ~~in the case of~~ calibration against storage. ~~While the~~The median KGE$_{storage}$ ~~in the case of~~ for calibration against storage anomaly ~~is slightly better than when calibrated against~~ exceeds that for estimated storage,

~~the widest box of~~ yet the letter-value plot ~~related to calibration against~~ shows the widest box for estimated storage, ~~which contains~~indicating 50% of the data~~,~~ is above ~~the one~~that for ~~calibration against~~ storage anomaly. ~~The improvement of storage~~Storage simulation ~~is mainly through~~improvement largely stems from bias adjustment (Fig. S3). The DH algorithm ~~has~~shows a median B_{KGE} of 1.90 ~~for storage~~ during ~~the~~ calibration~~ period. This value decreases~~, dropping to 0.92 (1.04, 0.99), 0.71 (0.91, 1.18), and 1.25 (1.44, 1.32) for ~~calibration~~calibrating against storage, storage anomaly, and estimated storage of the CH (SA, WA) ~~algorithm, respectively. The correlation is improved in the case of~~algorithms. Correlation improves for SA and WA ~~but~~ only ~~in the~~during calibration ~~period~~ (Fig. S2). ~~The variability is improved for calibration~~ Variability improves when calibrating against storage anomaly, ~~while calibration against~~whereas estimated storage ~~leads to an underestimation of storage~~underestimates variability (Fig. S4). ~~By calibration~~ Trends of $KGE_{storage}$ improve significantly when calibrating against storage, storage anomaly, and estimated storage~~, the trend component of $KGE_{storage}$ strongly improves as~~ compared to DH~~ for the calibration period but the trend is on average still~~, though trends are generally underestimated (Fig. S5). ~~Assessing the~~Evaluating $KGE_{storage\_anomaly}$ ~~when calibrating~~ with different variables shows less degradation ~~during~~in the validation phase (Fig. S6). For ~~example, the number of~~instance, skillful simulations for storage reached 17 (18), 93 (44), 98 (59), and 99 (55) ~~when calibrating using storage anomaly with DH, CH, SA, and WA, respectively (see Table 2 for comparison).~~for DH, CH, SA, and WA, respectively, when calibrated with storage anomalies (see Table 2 for comparison). The fit to observed storage variables is less improved for validation than calibration (Table 2, Fig. 2). Comparing calibration against storage anomaly and estimated storage shows SA and WA are preferred over CH and DH, even though the differences from CH are minor during validation. Differences between $KGE_{storage}$ values of SA and WA are small for all calibration variables in both calibration and validation periods.

~~The fit to observed storage-related variables is much less improved as compared to DH for the validation period than for the calibration period (Table 2 and Fig. 2). Comparing calibration against storage anomaly and estimated storage, which are the available options when using only remote sensing data, reveals that SA and WA are preferable to CH and DH, even though the differences from CH are small during the validation period. Differences between the $KGE_{storage}$ values of SA and WA are small for all calibration variables for both calibration and validation periods.~~

Examining the empirical cumulative distribution functions (eCDFs) for nRMSE reveals that the eCDFs for outflow are much closer across ~~different~~ algorithms ~~compared to~~than those for storage (see Fig. 3). This ~~suggests that~~implies calibration has a more significant impact on storage than on outflow. ~~Calibration~~Calibrating against any storage-related variable generally enhances outflow performance at lower $nRMSE_{outflow}$ levels ~~(~~in ~~approximately~~about 60% of ~~the~~ reservoirs~~), while~~. In comparison, at higher ~~$nRMSE_{outflow}$ ranges~~levels, a slight degradation ~~is observed~~occurs in ~~about~~roughly 35% of reservoirs (with probabilities ~~ranging from less than 0.60 to 0.95, mainly concentrated~~ between 0.~~8~~60 and 0.~~9~~95). When calibrating against outflow, ~~there is generally improvement in~~ $nRMSE_{storage}$ generally improves for CH and WA algorithms, ~~while~~but no clear ~~improvement~~enhancement is seen for SA. ~~Moreover, the error in outflow simulation is reduced in~~ Additionally, the $nRMSE_{outflow}$ decreases for over 40% of reservoirs~~ where the $nRMSE_{outflow}$ was already lower compared to others.~~. For $nRMSE_{outflow}$ greater than 0.98, ~~there is almost no discernible improvement observed when calibrating algorithms~~calibration against outflow shows nearly no improvement, as indicated by the eCDFs. ~~The calibration~~Calibration against the storage anomaly, ~~which is~~ the main calibration variant, especially in the validation phase, reveals that SA slightly ~~performs better than WA. SA shows~~ outperforms WA, with lower $nRMSE_{storage}$ ~~lower~~ and ~~nearly~~ similar $nRMSE_{outflow}$ ~~compared to WA. Disregarding~~. Regardless of the magnitude of the error, the eCDF for validation ~~has~~exhibits a shape similar to that of the calibration period, ~~suggesting~~indicating that the error distribution for the algorithm ~~is~~remains consistent across both periods.

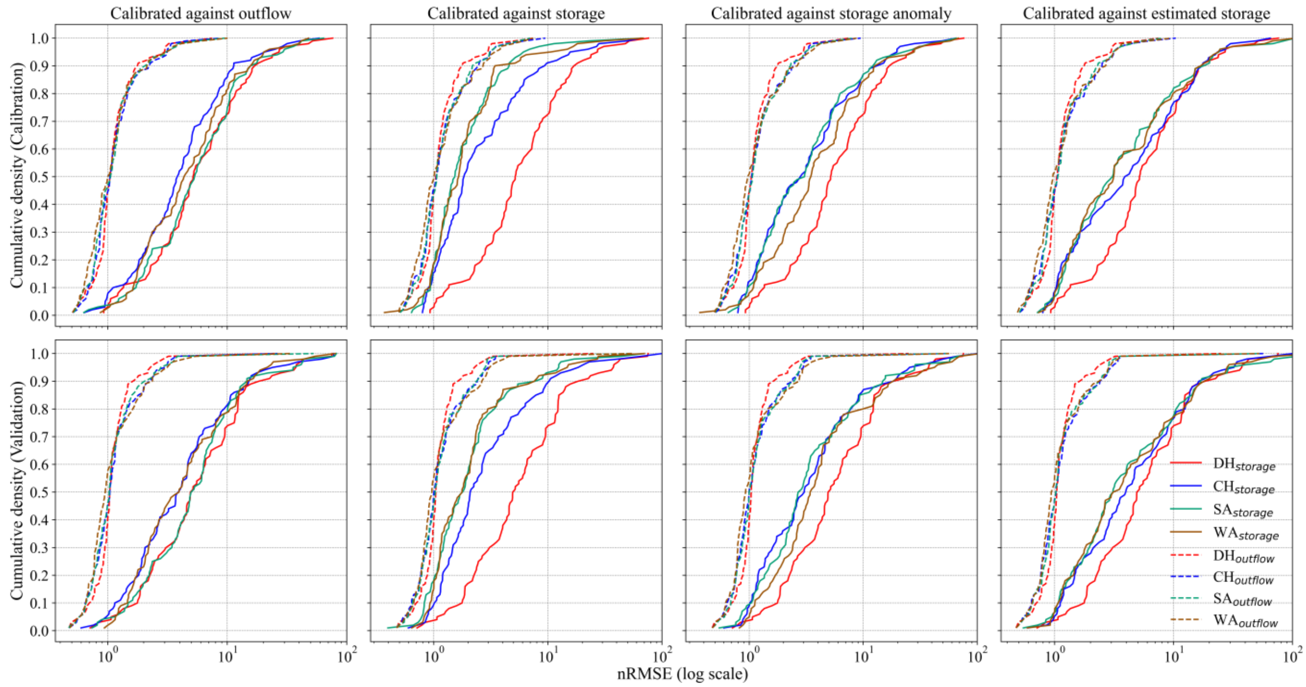

Figure 3. Empirical cumulative distribution functions of nRMSE for storage and outflow of the 100 studied reservoirs are based on the DH, CH, SA, and WA algorithms for the calibration period (1980-2009) and the validation period (2010-2019). All algorithms are calibrated against outflow (first column), storage (second column), storage anomaly (third column), and estimated storage (fourth column~~)~~), using KGE as the objective function. The x-axis ~~has~~uses a logarithmic scale. If nRMSE is ~~larger~~greater than 1, the mean error ~~is larger than~~exceeds the standard deviation of the observational values. The inflow data is sourced from the WaterGAP model.

3.2 Illustrative calibration results for three reservoirs

As an example, we plotted the time series of storage and outflow for the Glen Canyon Dam (Lake Powell) in ~~Fig~~Figs. 4 and ~~Fig.~~ S7, respectively. ~~This dam is one of the largest in our study, with several dams located upstream. The WaterGAP dataset includes four upstream reservoirs as global reservoirs, with storage capacities ranging from 0.57 to 4.3 km^3. Calibrating~~Results for this reservoir suggest that calibrating the H06 algorithm ~~against~~based on outflow did not ~~lead to~~yield better ~~results compared to~~ outcomes than the DH model (Fig. 4a, Fig. S7a). ~~However, some~~Some improvement was ~~observed~~noted in the outflow simulation for SA and WA during ~~the~~ calibration~~ period, though~~; however, this ~~led to~~resulted in a worse ~~outflow~~ simulation during ~~the~~ validation ~~phase~~ (Fig. S7). Despite this, with a KGE > -0.73, all outflow simulations demonstrated skillful performance. Calibration against outflow did not ~~degrade~~negatively impact storage simulation ~~compared~~relative to the DH, except for SA, particularly during ~~the~~ validation~~ phase~~, where the variability of the simulated ~~time~~ series was ~~more than~~over three times higher than the observed ~~one~~values (Table S3). During the calibration phase~~,~~ against storage-related variables, simulated storage levels ~~are mainly above~~primarily exceed 40% (10 km^3) of the total capacity~~, with a sharp decline between 40% and 70%, and smaller changes when the reservoir is filled above 70% (17.5 km^3).~~. This pattern ~~leads to~~results in storage levels ~~below~~under 40% ~~not~~ being ~~adequately considered in~~inadequately handled during the parameter selection ~~process. As a result~~for the SA and WA algorithms. Consequently, when storage ~~drops~~levels drop below 10 km^3 during the validation phase, the outcomes are not promising (~~Fig. 4). The large~~

~~difference~~Figs. 4c, 4d). Furthermore, the discrepancy between the ~~capacity~~ reported capacity by GRanD (25 km^3) and the maximum ~~observed~~recorded daily storage (31.7 km^3) ~~results in poorer performance in storage~~ negatively impacts the simulation outcomes for all calibrated algorithms ~~based~~that rely on estimated storage ~~compared to~~versus storage ~~anomaly~~anomalies (see Fig. S1). This ~~∼~~approximately 20% ~~difference~~discrepancy between the reported capacity and the maximum observed storage introduces a ~~20%~~ bias, which ~~directly impacts~~influences the bias and variability components of KGE$_{storage}$ (Table S3). ~~However, there is~~ The outflow shows almost no bias ~~in the outflow, thanks~~due to the use of data from the Lees Ferry station, located just downstream of the dam, ~~which is used in the~~for bias adjustment ~~of~~in WaterGAP's streamflow simulations ~~in WaterGAP through~~via a simple calibration approach~~.~~ (see Müller Schmied et al., 2024, for more details).

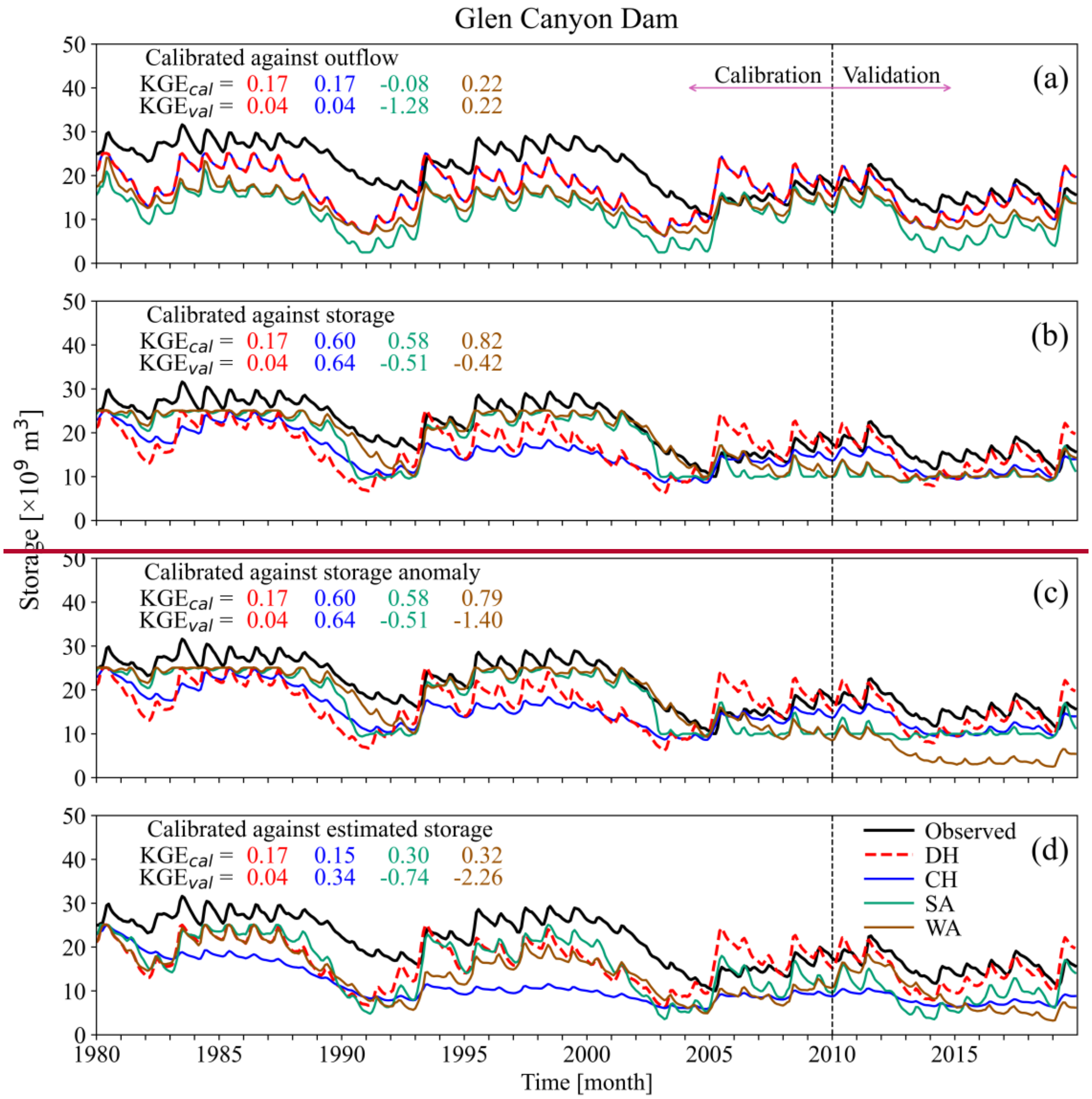

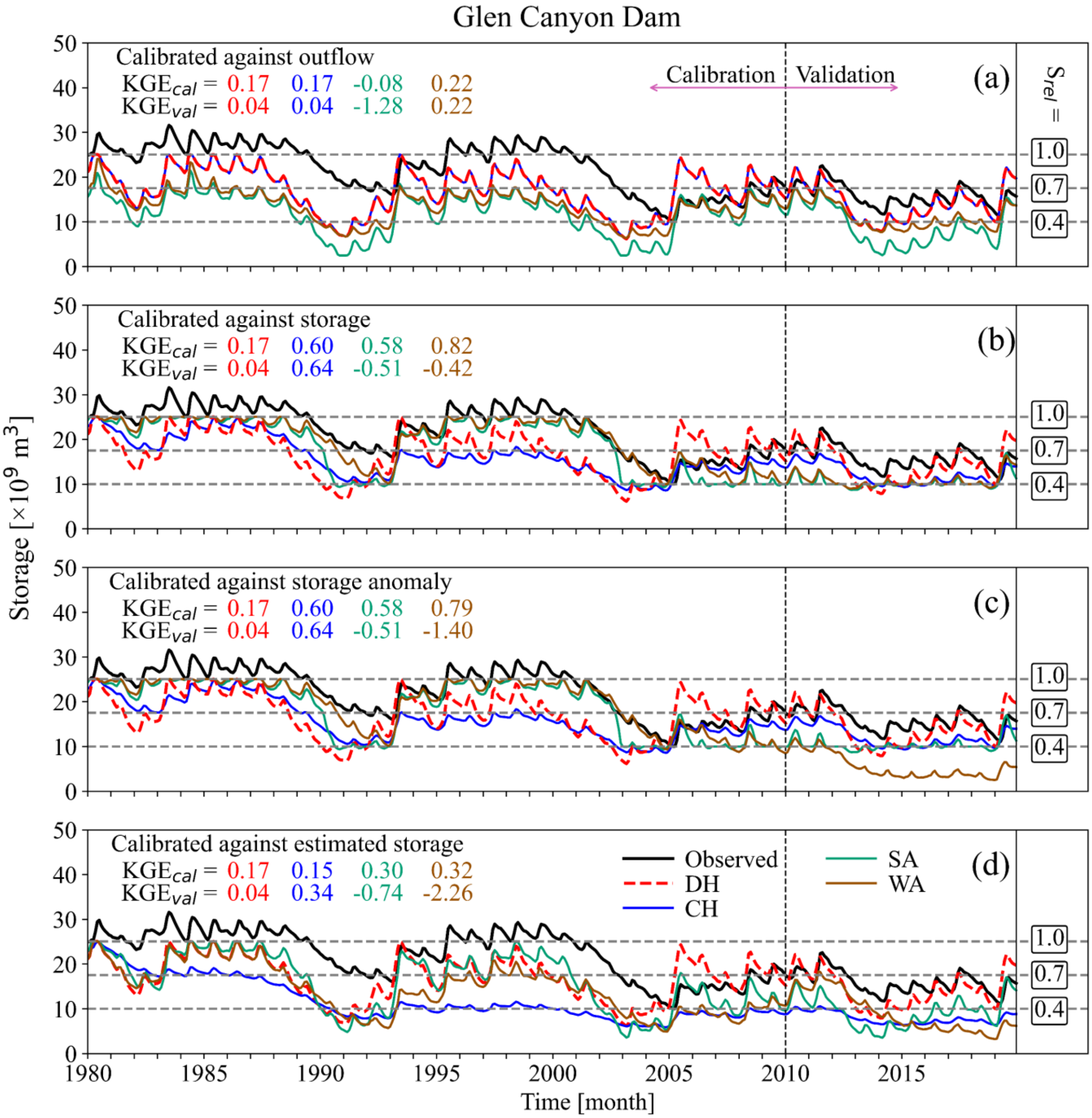

Figure 4. Monthly time series of observed and simulated storage values from DH, CH, SA, and WA algorithms for Glen Canyon dam, GRanD ID 597, calibrated against (a) outflow, (b) storage, (c) storage anomaly, and (d) estimated storage using KGE as the objective function. The dashed black lines distinguish between the calibration and validation periods. The dashed gray lines indicate the relative storage levels (S_{rel}), categorizing GRanD storage into three categories: above 70% of storage capacity, between 40% and 70% of storage capacity, and below 40% of storage capacity for the reservoir. The maximum observed storage (31.7 km^3) exceeds the capacity reported in the GRanD dataset (25 km^3). The inflow data is sourced from the WaterGAP model. The time series for outflow is plotted in Figure S7.

~~Very poor~~The storage simulation ~~with a much higher seasonal magnitude compared to observed storage is seen~~ for the Yellowtail Dam (~~GRanD ID = 355),~~ an irrigation reservoir~~ with different calculations in the DH~~, GRanD ID = 355) and ~~CH algorithms compared to the SA and WA algorithms, and for~~ the Harry S. Truman Dam (~~GRanD ID = 989), which is~~ a hydropower reservoir, GRanD ID = 989) is poor, with a higher seasonal magnitude compared to the observed data. (Fig.

5). Calibrating ~~against~~using storage anomaly can ~~lead to time series of storage with considerable~~introduce significant bias in absolute storage simulation (Fig. 5c). ~~This issue can also occur when~~Similarly, calibrating ~~against~~with estimated storage may cause issues if there is ~~an offset between the estimated storage and the~~ a mismatch with in-situ ~~observation~~observations (Fig. 4d). ~~The time series related to~~For the Yellowtail Reservoir ~~reveals that~~, SA and WA, which do not ~~consider the irrigation purpose of this reservoir, can~~account for downstream water demand, simulate ~~reservoir~~ storage ~~better~~more accurately than DH and CH, which ~~explicitly take into account the~~consider downstream water demand (Fig. 5a). However, ~~the opposite is true~~ for outflow simulation, ~~where~~ the uncalibrated DH performs the best (Fig. S8a).

~~From these~~These examples~~, we found~~ show that calibrating ~~solely~~only against storage ~~related~~ variables does not necessarily ~~lead to poorer~~worsen outflow simulations (Fig. S8). However, ~~other factors, such as~~attention to inaccuracies in reservoir capacity data ~~(e.g., for the Glen Canyon Dam) and discrepancies between actual available water and the reported static storage value~~ in the GRanD dataset ~~— which may include dead storage (see Table S1 for Yellowtail and Harry S. Truman dams) — are important considerations~~is critical when evaluating ~~the performance of the~~ reservoir operation ~~algorithm~~performance. In ~~such~~these cases, comparing storage ~~anomaly~~anomalies may ~~offer~~provide a more ~~reasonable~~accurate assessment than ~~comparing~~relying solely on absolute storage. This storage simulation error ~~in storage simulation~~ may also ~~affect~~impact outflow simulations, where input data inaccuracies ~~in input data are the primary factor leading to inaccurate~~primarily lead to incorrect storage levels ~~being maintained~~ during the validation phase (Fig. 4c).

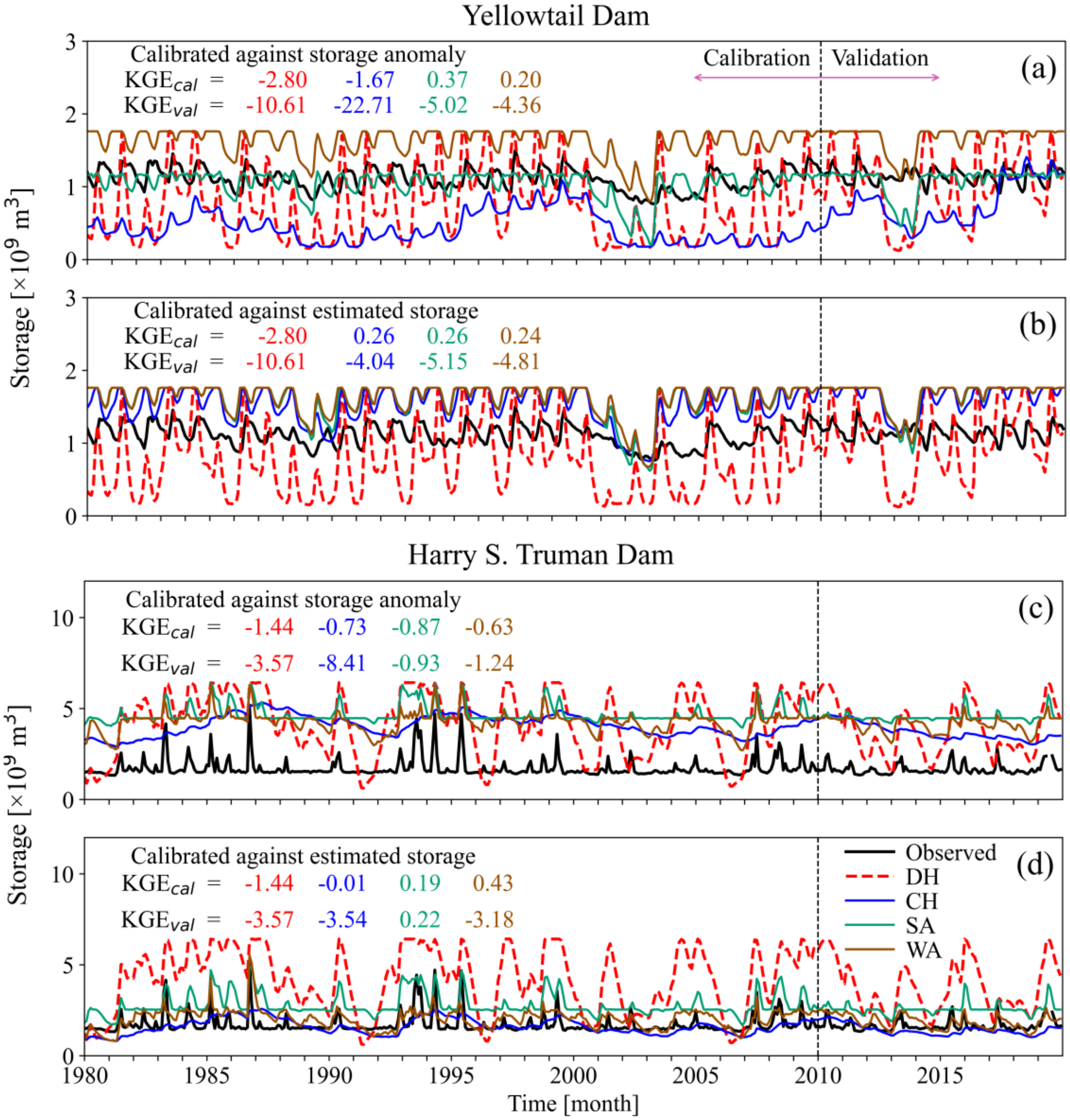

Figure 5. Monthly time series of observed and simulated storage values from DH, CH, SA, and WA algorithms for Yellowtail/Harry S. Truman reservoirs, GRanD IDs 355/989, calibrated against (a, c) storage anomaly and (b, d) estimated storage using KGE as the objective function. The primary purposes of the Yellowtail Dam and the Harry S. Truman Dam are irrigation and hydropower, respectively. The dashed black lines distinguish between the calibration and validation periods. The inflow data is sourced from the WaterGAP model. The time series for outflow is plotted in Figure S8.

3.3 Impact of using observed streamflow as input to the reservoir operation algorithms

~~Comparing the results~~ The comparison of ~~the~~ modeling results using WaterGAP inflow and observed inflow is ~~presented~~shown in Fig. 6 for 35 ~~reservoirs~~out of the 100 studied ~~ones. Based on~~reservoirs. Fig. 6~~, there is~~ shows no ~~overall improvement or deterioration~~considerable change in storage simulation ~~when using~~with either observed or WaterGAP inflow data, except for the WA algorithm, which ~~demonstrates~~performs better ~~performance~~ with observed inflow than with simulated ~~streamflow. This is evident as most of the circles are positioned above the y=x line~~ inflow (Fig. 6c). ~~However,~~ Nonetheless, the performance of WA in storage simulation with observed inflow ~~is~~does not ~~better than the~~

~~performance~~exceed that of SA. ~~In contrast, there is a considerable improvement in~~Conversely, using observed inflow data considerably enhances the reservoir outflow simulation ~~when utilizing observed inflow data~~. For instance, KGE$_{outflow}$ below -1 achieved with WaterGAP inflow can approach 1 with observed inflow (Fig. 6f). In most cases, KGE$_{outflow}$ between 0-0.5 based on WaterGAP inflow reaches 0.5-1 based on observed inflow. The most substantial improvement is ~~observed for~~seen in the WA algorithm, where the median of KGE$_{outflow}$ across various calibration objectives, ranging from [-0.27, 0.14], ~~increases~~rises to [0.56, 0.69] upon replacing WaterGAP inflow with observed data. ~~It~~This implies that the WA is more sensitive to the quality of inflow data than other algorithms. ~~The same pattern is reiterated during~~During the validation period, ~~with the~~ the same pattern is repeated, showing a median KGE$_{outflow}$ of [0.38, 0.56] compared to [-0.87, -0.41~~]~~], based on observed inflow ~~compared to~~versus WaterGAP inflow across all calibration variants (Fig. S9). ~~Using~~ Utilizing the observed inflow ~~improves almost~~enhances nearly all components of KGE$_{outflow}$, ~~but the main components that are improved are~~with the most notable improvements seen in the variability and trend components (see Figs. S10-S17).

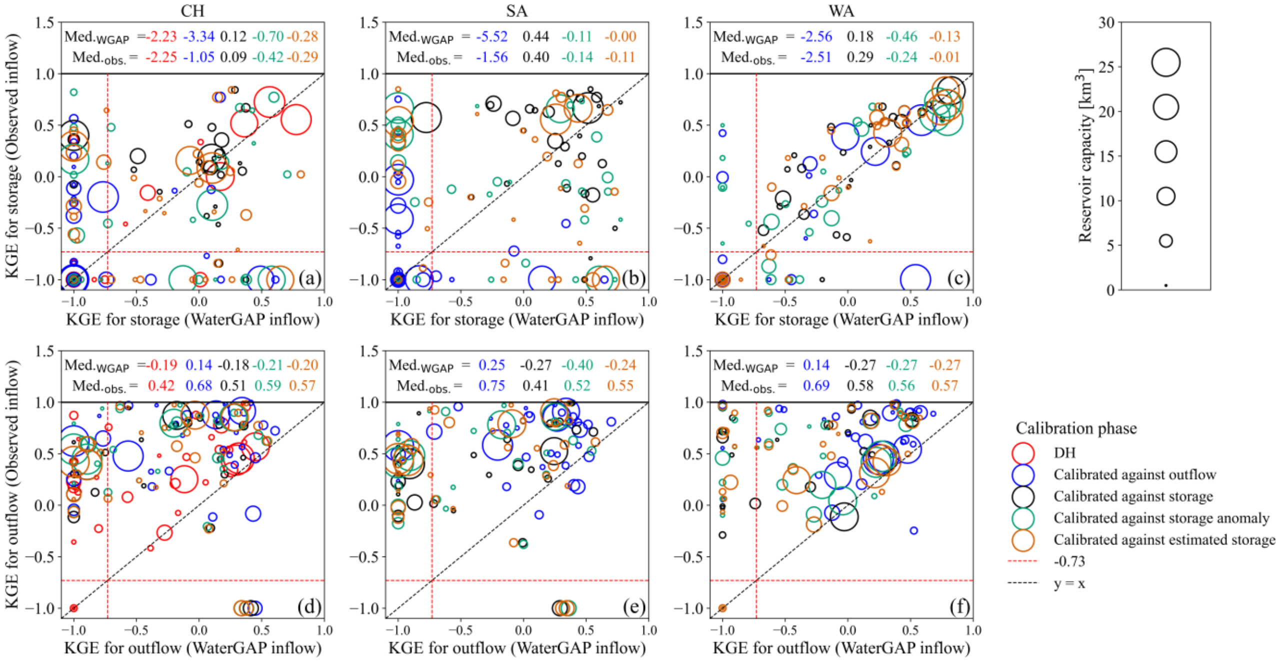

Figure 6. The relationship between the KGE of (a-c) storage and (d-f) outflow is obtained from modeling reservoirs using WaterGAP inflow and the observed inflow to the reservoirs ~~for~~during the calibration period (1980-2009) for 35 reservoirs with observed inflow. KGE values less than -1 are set to -1. The KGE values for storage anomaly and estimated storage are not ~~shown~~displayed. The ~~circle~~ size of the circles indicates the reservoir capacity. The values above each panel ~~indicate~~show the median KGE, with the top values achieved with WaterGAP inflow and the bottom values ~~with~~derived from observed inflow. The dashed red lines ~~indicate~~represent the KGE benchmark threshold of -0.73.

3.4 Impact of considering downstream water demand

We ~~evaluated~~assessed the ~~benefit~~advantages of ~~distinguishing~~differentiating irrigation and water supply reservoirs from others by counting how many times estimating the outflow of irrigation reservoirs (9 reservoirs) and supply reservoirs (12 reservoirs) using Eq. 4 ~~(the default approach for irrigation reservoirs~~results in ~~the H06 algorithm, which takes into account~~

~~the seasonality of downstream water demand) leads to~~ a more ~~skillful~~accurate simulation compared to ~~disregarding~~ignoring water demand in the modeling of reservoir dynamics. We found that there is no general advantage in distinguishing irrigation and supply reservoirs from other reservoirs, ~~in particular~~particularly when calibrating against storage anomaly or estimated storage using the overall superior WA and SA algorithms. ~~While in the case~~In terms of calibration against estimated storage, the SA algorithm performs better for outflow ~~with~~when considering downstream demand; however, the opposite is true for storage. ~~For~~In the WA algorithm, the same number of reservoirs achieve better or worse streamflow performance ~~if taking into account~~when downstream water demand ~~while~~is considered. However, storage performance is ~~better if~~enhanced when demand is ~~not considered~~disregarded (Table 3).

Table 3. ~~The number~~Comparison of ~~irrigation and supply reservoirs (out of 21) where KGE values for the calibration phase are higher when~~ reservoir simulation performance using different algorithms, both with and without considering downstream water demand ~~than when neglecting downstream demand. Improvements are only identified if the achieved KGE value is larger than -0.73, i.e. the simulation is skillful. The values in~~for 21 irrigation and supply reservoirs. Numbers outside parentheses indicate the number of reservoirs (out of 21) where performance improves when downstream demand is taken into account. In contrast, values inside parentheses represent reservoirs where ~~neglecting~~ignoring downstream demand leads to higher KGE values. Improvements are noted only for skillful simulations achieving a KGE value greater than -0.73. All algorithms are calibrated against outflow, storage, storage anomaly, and estimated storage using KGE as the objective function. The inflow data is sourced from the WaterGAP model.

Calibrated variable	CH		SA		WA	
	Outflow	Storage	Outflow	Storage	Outflow	Storage
Outflow	4 (5)	1 (3)	10 (6)	1 (3)	8 (8)	3 (4)
Storage	7 (6)	7 (2)	5 (6)	11 (10)	6 (6)	7 (14)
Storage anomaly	6 (6)	3 (3)	7 (6)	7 (10)	8 (6)	7 (9)
Estimated storage	6 (4)	6 (1)	9 (3)	6 (10)	6 (6)	3 (12)

4 Discussion

4.1 Calibration variables

Calibrating against outflow does not necessarily improve storage simulations and may even ~~lead to~~cause their ~~degradation~~deterioration during the calibration phase. In contrast, calibrating against all types of storage-related variables slightly improves outflow compared to the DH algorithm (see Fig. 2 and Table 2). Thus, calibrating against storage-related variables is more effective than calibrating against outflow when aiming to improve the simulation of both variables through a single-objective calibration. ~~Additionally, comparing~~Furthermore, an analysis of the KGE values ~~of~~for the compromise solution ~~(~~—defined as the ~~solution~~one with the ~~minimum~~smallest Euclidean distance from the ~~optimal~~ideal KGE value of 1 for both storage and outflow ~~) with KGE values from calibrations against storage and outflow indicate~~ —reveals that the KGE results ~~of~~from calibration against storage are considerably closer to the compromise solution ~~compared to~~than those for outflow (~~see~~refer to Fig. S18). A similar pattern is ~~observed for~~seen in calibrations against both storage anomaly and estimated storage. ~~This suggests that calibrating solely against storage-related variables yields results closer to the compromise solution than calibrating against outflow alone.~~ One reason for this is ~~the lower sensitivity of~~ that outflow simulations are less sensitive to calibration compared to storage simulations. This finding is encouraging because, unlike outflow data, storage anomaly can be estimated using remotely sensed data. The data length should exceed five years to be used effectively for this purpose (Otta et al., 2023). Although our results indicate that, in general, calibrating against storage anomaly improves the simulation of storage, using the absolute simulated storage from ~~such calibrations should be done carefully, as~~ these calibrations should be approached with caution, as they do not always ~~guarantee~~ensure an improvement in absolute storage.

Calibrating against estimated storage does not outperform calibrating against storage anomaly (see Fig. 2 and Table 2~~), although~~). Although theoretically, it should ~~provide~~yield results closer to ~~calibration~~those of calibrating against actual storage. The reason~~ for this, besides the~~, aside from inherent ~~error in~~ storage estimation~~, can be traced to~~ errors, lies in the discrepancies between ~~the~~GRanD's capacity ~~information from GRanD~~ data and the maximum daily ~~observed~~recorded storage~~ (~~, with a median difference ~~equals to ~25%). The maximum observed storage should be less than or equal to capacity unless during an overtopping period. However, comparing maximum daily storage data from ResOpsUS with reservoir capacity from GRanD shows notable differences in several cases (see~~ of about 25% (refer to Table S1). Steyaert and Condon (2024) also reported that~~, due to~~ GRanD's omission of overtopping and potential ~~inclusion of~~ inaccurate data~~,~~ led to 100 ~~out~~ of the 679 dams ~~listed~~ in the ResOpsUS dataset ~~have~~having maximum storage values exceeding the reservoir capacities reported by GRanD. Inconsistencies are also reported for the reservoir area; Dong et al. (2023) ~~reported~~indicated that the actual ~~reservoir~~ polygons of Ertan ~~Reservoir~~ and Jinping I ~~Reservoir~~Reservoirs are 69% and 50% larger, respectively, than the GRanD polygons. ~~Therefore, for those reservoirs, modeling reservoir~~ Consequently, simulating the operation ~~using~~of reservoirs that have inaccurate GRanD ~~information should not lead~~data is unlikely to ~~good~~yield favorable results, ~~particularly for~~especially in terms of absolute storage simulation. ~~Consequently,~~ Thus, an absolute storage comparison may not be a fair approach for assessing model performance~~ assessment~~, although it ~~remains valid~~still holds validity for comparing different algorithms. An ~~assessment~~evaluation of the degradation in KGE values~~ obtained from~~, comparing calibration against estimated storage ~~compared to~~with calibration against actual storage~~ reveals~~, indicates that the results from estimated storage align closely ~~match~~with those from actual storage when the ~~difference~~discrepancy between the reservoir capacity reported by GRanD and the maximum daily observed storage is minimal. ~~However, as~~As this difference increases, the discrepancy between the results of the two calibration variants also grows (Fig. S19). It is important to note that ~~calibration~~calibrating against storage anomaly does not ~~exhibit~~show a direct relationship with these differences in ~~storages~~storage.

To the best of our knowledge, there are currently two global datasets — the Global Reservoir Storage (GRS) introduced by Li et al. (2023) and the GloLakes dataset by Hou et al. (2024) — that provide monthly time series of estimated absolute storage using remotely sensed information, along with either a geostatistical model or a volume-elevation/area-volume relationship. We ~~assessed~~evaluated the quality of their estimates for the absolute storage of the studied reservoirs. GRS covers all 100 studied reservoirs, while GloLakes includes only 57 of those ~~100~~ reservoirs. The median KGE$_{storage}$ (without the trend component) was 0.26 for GRS and 0.14 for GloLakes, ~~indicating~~showing that neither dataset ~~provides~~ offers reliable estimates ~~accurate enough to be considered reliable~~ for calibrating reservoir operation algorithms ~~against their estimated~~based on absolute storage (see Table S4). The BKGE components for GRS~~, with~~ exhibit a median of 0.84, ~~range~~varying from ~~significant~~marked underestimation~~ — such as~~ — for example, at Norfork Dam (GRanD ID 1042), ~~where~~ the ~~mean~~average estimated storage is ~~only~~merely 2% of the observed value~~ —~~ — to ~~substantial~~considerable overestimation, ~~such~~ as ~~for~~seen at Albeni Falls Dam (GRanD ID 305), where the ~~mean~~average estimated storage is 45 times ~~greater than~~ the observed value. GloLakes, with a median B_{KGE} of 1.49, performs slightly better in terms of extreme bias; the ~~largest~~most considerable underestimation occurs at Santa Rosa Dam (GRanD ID 1086), where the mean estimated storage is only 35%

of the observed value. ~~Maximum~~The maximum overestimation for GloLakes is observed at the same dam (Albeni Falls Dam~~)~~), but it is less extreme compared to GRS, ~~though~~although still substantial. The R_{KGE} and V_{KGE} components of KGE for storage are better than B_{KGE} in terms of extreme values. ~~However~~Nonetheless, with medians of 0.63 and 0.84 for GRS and 0.71 and 0.47 for GloLakes, respectively, R_{KGE} and V_{KGE} for both datasets are still not sufficiently promising, indicating uncertainty in estimates of remotely sensed storage ~~anomaly estimates~~anomalies.

4.2 Value of calibration and choice of reservoir operation algorithm

~~Applying~~By using streamflow ~~simulated by~~from the global hydrological model WaterGAP 2.2e as inflow to 100 US reservoirs, we found that the outflow generated by the calibration-free algorithm DH is a better alternative to the mean observed outflow. ~~However~~Conversely, the opposite ~~is true~~holds for simulated reservoir storage (see Fig. 2), ~~underscoring~~highlighting the need for reservoir-specific calibration. Our findings ~~indicate that~~show all three calibrated algorithms generally perform better than DH ~~in terms of~~for storage, but ~~the~~their effect on reservoir outflow simulation is negligible. ~~The degree of improvement varies considerably~~Improvements vary substantially between reservoirs, ~~and in~~with some ~~cases, no improvements are seen~~showing none, as ~~also reported~~noted by Turner et al. (2021) with a more complex reservoir operation algorithm. Among ~~the~~ calibrated algorithms, SA and WA ~~performs better than~~outperform CH when calibrated against storage~~, storage anomaly, and estimated storage. Thus,~~ related variables. CH may ~~only~~ be preferred over SA and WA ~~in the case of~~for irrigation reservoirs with rather good water demand ~~information~~data or if computational resources are very limited, as ~~CH requires the estimation of~~it estimates only two parameters instead of three ~~parameters~~ for non-irrigation reservoirs. ~~While~~Although KGE cannot distinguish the performance of SA and WA ~~cannot be distinguished by KGE~~, nRMSE ~~indicates a~~ suggests that SA performs slightly better ~~performance of SA in the case of calibration~~when calibrated against storage anomaly (Fig. 3).

Calibration of H06 ~~reveals~~shows that default parameters are rarely included in the calibrated ~~parameter~~ sets (Fig. S20), ~~especially noticeable~~particularly for irrigation reservoirs, where parameter a_2 almost always remains at ~~its~~the lower bound of 0.1. According to Eq. 4, this ~~implies~~suggests that calibration ~~prioritizes using~~ emphasizes the use of a scaled version of long-term inflow ~~rather than~~instead of directly integrating demand through addition. The demand estimation is not accurate enough for reservoir operations, ~~resulting in increased~~which increases complexity with limited ~~benefit~~benefits when distinguishing irrigation and supply reservoirs from other types of reservoirs (Table 3). Vanderkelen et al. (2022) similarly observed minimal additional value in ~~including~~incorporating irrigation demand ~~in~~into the reservoir operations.

4.3 Relevance of the quality of simulated reservoir inflow and reservoir storage capacity data

We found that ~~the quality of~~ inflow data quality is more ~~important~~crucial than ~~the~~ reservoir operation algorithms for outflow simulation, ~~while it~~but has less impact on storage simulation. This finding aligns with Vanderkelen et al. (2022), who attributed the similar performance of natural lake parameterization and H06 to ~~poor~~poorly simulated streamflow in the Community Land Model. ~~Using~~Comparing observed inflow as a substitute for simulated outflow ~~(ignoring the dam) and comparing it with~~and observed outflow ~~reveals~~shows that the DH algorithm~~, with median $KGE_{outflow}$ values of 0.42 (calibration) and 0.02 (validation), results in~~ generates worse outflow simulations compared to ignoring the ~~observed inflow, which~~dam. DH has median $KGE_{outflow}$ values of 0.42 (calibration) and 0.02 (validation) while observed inflow shows median KGE$_{outflow}$ values of 0.57 (calibration) and 0.36 (validation). This ~~is in line~~aligns with Vora et al. (2024), who reported that ignoring reservoirs in modeling may lead to better outflow simulations than DH in some cases. However, some skill is observed in other algorithms, particularly SA, where the median KGE$_{outflow}$ values for CH, SA, and WA are 0.68 (0.46), 0.75 (0.52), and 0.69 (0.56) for calibration (validation), respectively, when calibrated against outflow (see Figs. 6 and S9). ~~In contrast to~~ Unlike Vanderkelen et al. (2022), our study ~~found~~showed that ~~using~~ observed inflow did not ~~lead to a clear improvement in~~significantly improve storage simulation. ~~One possible reason is the error~~This may be due to errors in GRanD data, ~~with~~which has a median difference of ~~\~~~about 14% ~~between GRanD data and~~from the maximum daily observed storage for reservoirs with observed inflow data. Another ~~potential~~possible reason ~~could~~might be the ~~impact~~influence of initial storage on simulation ~~outcomes~~results, which ~~varies depending~~differs based on the ~~level of~~ regulatory level of reservoir operations, as ~~reported~~stated by Yassin et al. (2019). In summary, our results suggest that enhancing the quality of inflow data is more crucial than calibrating reservoir operation algorithms, particularly when the objective is to achieve accurate outflow simulation. Only calibrating against storage ~~anomaly as the main calibration variant will~~anomalies does not ~~result in accurate outflow simulations unless the quality of inflow data is significantly improved~~ensure better outflow predictions.

4.4 Complexities of reservoir operations and dynamics

~~In addition to~~Besides poor inflow data and inaccurate capacity information, other factors also ~~impact~~affect the performance of reservoir operation algorithms. Incorporating human decision-making into the model is very challenging, despite its critical importance (Rougé et al., 2021). This complexity arises because human decisions do not always follow operational rules due to ~~evolving~~changing conditions, such as ~~changes~~variations in water demand (Shah et al., 2019) or during droughts and floods (Nazemi and Wheater, 2015). For example, the Hoover Dam (Lake Mead) and Glen Canyon Dam (Lake Powell) are interconnected, and historically, Glen Canyon could release enough water to meet downstream needs until 2014. However, due to a drought in 2012 and 2013, ~~the release~~releases from Glen Canyon Dam in 2014 dropped to ~~its~~the lowest level since the initial filling of Lake Powell in 1963 (Arizona Water Resource, 2013; Colorado River Drought, 2019). This reduction in release ~~was~~ aimed ~~at recovering~~to recover Lake Powell's storage, which had fallen to ~~\~~~around 40% of its capacity (NASA Earth Observatory, 2014). Additionally, climate change and increases in water demand can ~~lead to~~result in non-stationary situations, meaning that calibrated algorithms may not perform as well compared to the calibration period. This trend is observed in the ResOpsUS dataset, where there is a generally ~~a~~ decreasing trend in reservoir storage, which also impacts release (Steyaert and Condon, 2024). For example, the Hoover Dam has experienced a continuous negative trend in its ~~capacity~~storage since 2000 (see Fig. S21). Understanding these trends is crucial for assessing the degradation of the studied algorithms during the validation period, where the connection between observed inflow and outflow also becomes weaker.

4.5 Limitations

~~In this~~This study~~, we~~ modeled ~~each reservoir~~ reservoirs independently, which may ~~affect the quality of the~~ have potentially affected analysis~~. In practice, a~~ quality. A calibrated upstream reservoir ~~would lead to different~~can alter inflows to ~~a~~the downstream reservoir. ~~However, since~~ Nevertheless, as the calibration has not ~~had a considerable impact on~~significantly influenced the outflow simulation, it is expected that the overall conclusions ~~would be similar. For~~will remain comparable.

In the case of the SA and WA algorithms, a reservoir ~~may reach~~might attain relative storage ~~level(s) (see~~levels (refer to Eqs. 7 and 8) during the validation phase that were not observed during the entire calibration period. ~~Consequently~~As a result, the parameters for these ~~unseen~~unobserved relative storage levels ~~cannot be determined~~remain indeterminate and are ~~set to~~assigned the ~~lowest~~minimum value (0.1 for both SA and WA). As a result, the performance of the algorithm for those reservoirs during the validation phase is ~~affected~~influenced by setting these undetermined parameters to ~~the~~their lowest value. In the case of the SA algorithm, this issue ~~occurs for~~affects at most four reservoirs across the calibration variants, while for the WA algorithm, it ~~occurs for~~impacts up to nine reservoirs (see Table S5). ~~Moreover, although~~ Yassin et al. (2019) ~~suggest~~indicate that a five-year spin-up period is generally sufficient ~~to fully stabilize~~for complete stabilization, even for large dams~~, and~~. In our study, we ~~used~~conducted five simulations of 1979 as our spin-up period~~,~~. However, using a longer ~~run extending further back~~spin-up duration before 1980 could result in different initial storage conditions. Consequently, this ~~could~~might affect the performance of the operational algorithm. ~~This~~These potential ~~limitation~~limitations should be acknowledged, as ~~it~~they may ~~impact~~influence the accuracy and generalizability of the results.

5 Conclusions

~~In this~~This study~~, we~~ assessed whether monthly time series of observed reservoir storage ~~anomaly, which, unlike time series of storage and outflow, are~~anomalies, available ~~for many reservoirs worldwide from~~globally via remote sensing, are suitable ~~as~~ targets for calibrating reservoir operation algorithms in large-scale hydrological models. To ~~achieve~~accomplish this, we ~~integrated a~~incorporated the well-established ~~reservoir~~Hanasaki algorithm ~~and~~along with two ~~newly developed~~new ones, namely, WA and SA, into the global hydrological model WaterGAP~~, calibrating~~. We calibrated them against storage anomaly, estimated storage, storage, and outflow data ~~sourced~~ from ResOpsUS for 100 U.S. reservoirs. For 35 of these reservoirs ~~in the USA. For 35 out of the 100 reservoirs with available~~with observed inflow data, both observed and simulated inflows were ~~used~~included in the analysis. Our findings lead to the following conclusions:

- Using observed storage-related variables, i.e., storage anomaly, estimated storage, or storage, ~~for calibration of the~~to calibrate reservoir algorithms results in a clear improvement in storage simulation and ~~a slight improvement in~~slightly enhances outflow simulation during ~~the~~ calibration~~ phase, particularly when calibration is performed~~, especially against storage. However, the performance of the algorithms for storage during ~~the~~ validation ~~phase remains worse than their performance regarding outflow. It should be noted~~is still inferior to that ~~calibration using the rarely available~~for outflow. Calibration with scarce outflow data ~~leads to improvements~~improves only ~~in~~the simulated outflow~~ and does not noticeably affect~~, leaving the simulated storage~~, which remains very~~ distinctly poor.
- ~~Among~~Of the three calibrated reservoir operation algorithms, the two ~~newly introduced~~new algorithms, WA and SA, perform similarly ~~and~~or better in storage simulation than CH, i.e., the calibrated~~ version of the~~ Hanasaki algorithm.
- If observations of either storage, storage anomaly or outflow are available for a reservoir, the parameters of the reservoir algorithm should be adjusted, as we found that the default parameter set of the DH algorithm, particularly the irrigation reservoir parameter, is seldom the optimal ~~parameter~~ set. For~~ the~~ reservoirs without observations, a calibration-free algorithm such as DH has to be used.

- ~~Considering water demand in the modeling of~~Modeling irrigation and ~~water~~ supply reservoirs with water demand, as ~~done~~ in DH, ~~does~~may not ~~necessarily improve~~enhance reservoir simulation~~, potentially~~ due to ~~high~~ uncertainty in demand estimation. We ~~therefore~~ recommend ~~disregarding~~ignoring downstream water demand~~, even in the case of irrigation and water supply~~ for these reservoirs.
- We found that using observed inflow instead of simulated inflow considerably improves the performance of the reservoir operation algorithms ~~in terms of~~regarding outflow simulation, ~~but~~although it ~~does not have much~~has minimal impact on their performance in storage simulation.
- For ~~most~~many reservoirs, none of the three relatively simple reservoir operation algorithms can accurately ~~represent~~depict the dynamics of both ~~reservoir~~ outflow and storage, ~~even after~~despite calibration ~~against~~with observations of outflow or storage-related variables and ~~even with~~using observed inflow ~~used~~ in the simulation. The complexity of human decision-making ~~cannot be captured by~~eludes algorithms that rely solely on globally available information, even ~~if their~~when parameters are adjusted through calibration.
- To ~~improve~~enhance large-scale hydrological modeling, we ~~suggest leveraging~~recommend utilizing recent and upcoming spaceborne ~~information~~data on reservoir water storage ~~anomaly~~anomalies by ~~implementing~~employing the SA or WA reservoir operation algorithms~~, which enables~~. These algorithms facilitate reservoir-specific calibration against observed storage ~~anomaly. These algorithms showed, after~~anomalies. After calibration, ~~a~~they demonstrated slightly ~~better~~improved performance ~~than~~over the CH algorithm and are more ~~suitable~~suited for large-scale applications ~~than~~compared to algorithms ~~such as~~like those ~~of~~from Chen et al. (2022) and Turner et al. (2021~~) that~~), which require daily inflow, storage, and outflow data~~ — data that are rarely available~~ — information that's seldom accessible outside the US.
- ~~As~~Due to the strong biases often exhibited by the currently available time series of absolute reservoir storage derived from remote sensing-based water storage anomaly~~ often exhibit strong biases~~, and considering that calibration against estimated storage ~~did~~does not outperform calibration against storage anomaly, we recommend ~~to estimate~~estimating the parameters of the SA or WA algorithm using globally available, remote sensing-based monthly time series of reservoir water storage anomaly (and in-situ storage and outflow ~~–~~time series where available). This approach is expected to particularly enhance the quality of simulated reservoir storage.

~~Improving~~Although the algorithms introduced in this study outperform the conventional DH algorithm, there remains scope for improvement. For example, integrating knowledge-based equations with deep learning in hybrid machine learning methods could be beneficial for simulating reservoir dynamics. However, improving the accuracy of inflow simulations and validating reservoir-related characteristics ~~are considered~~is very likely more important for achieving better reservoir outflow and storage simulations than ~~solely improving~~refining the algorithm itself~~. Nevertheless, hybrid machine learning approaches, e.g. combining knowledge-based equations with deep learning, should be investigated for simulating reservoir dynamics. Finally, to further evaluate the impact of calibration approaches on the performance of reservoir operation algorithms, we suggest using more advanced parameter optimization methods than the grid search method we applied in this study.~~

Code availability. The WaterGAP 2.2e code is accessible through Müller Schmied et al. (2023) and is licensed under the GNU Lesser General Public License version 3.

Data availability. All storage and outflow data obtained from different algorithms and calibration variants, as well as the calibrated parameters, are available in the supplement as Excel files. The reservoir characteristics are provided in Table S1. The observed data are available through Steyaert et al. (2022).

Supplement. The supplement related to this article is available online at [URL].

Author contributions. SMHM and PD designed the study. SMHM performed the modeling and wrote the first draft of the manuscript. PD contributed to the result analysis and editing of the paper. Both SMHM and PD were primarily responsible for writing the paper.

Competing interests. The authors declare that they have no conflict of interest.

Acknowledgements. This study was supported by funding from the German Research Foundation for the research unit "Understanding the global freshwater system by combining geodetic and remote sensing information with modeling using a calibration/data assimilation approach (GlobalCDA)". We acknowledge ChatGPT's assistance with editing certain sentences, while the authors have reviewed and refined the content and assume full responsibility for the publication.

References

Arizona Water Resources: https://wrrc.arizona.edu/publication/arizona-water-resource-fall-2013, last access: 20 August 2024.

Beck, H. E., Pan, M., Roy, T., Weedon, G. P., Pappenberger, F., van Dijk, A. I. J. M., Huffman, G. J., Adler, R. F., and Wood, E. F.: Daily evaluation of 26 precipitation datasets using Stage-IV gauge-radar data for the CONUS, Hydrol. Earth Syst. Sci., 23, 207–224, doi: 10.5194/hess-23-207-2019, 2019.

Best, J.: Anthropogenic stresses on the world's big rivers, Nat. Geosci., 12 (1), 7–21, doi: 10.1038/s41561-018-0262-x, 2019.

Biancamaria, S., Lettenmaier, D. P., and Pavelsky, T. M.: The SWOT Mission and Its Capabilities for Land Hydrology, Surv. Geophys., 37, 307–337, doi: 10.1007/s10712-015-9346-y, 2016.

Chao, B. F., Wu, Y. H., and Li, Y. S.: Impact of artificial reservoir water impoundment on global sea level, Science, 320(5873), 212-214, doi: 10.1126/science.1154580, 2008.

Chen, Y., Li, D., Zhao, Q., and Cai, X.: Developing a generic data-driven reservoir operation model, Adv. Water Resour., 167, 104274, doi: 10.1016/j.advwatres.2022.104274, 2022.

Colorado River Drought: https://www.doi.gov/ocl/colorado-river-drought, last access: 20 August 2024.

Cooley, S. W., Ryan, J. C., and Smith, L. C.: Human alteration of global surface water storage variability, Nature, 591(7848), 78-81, doi: 10.1038/s41586-023-06165-7, 2021.

Dang, T. D., Chowdhury, A. F. M. K., and Galelli, S.: On the representation of water reservoir storage and operations in large-scale hydrological models: implications on model parameterization and climate change impact assessments, Hydrol. Earth Syst. Sci., 24, 397–416, doi: 10.5194/hess-24-397-2020, 2020.

Döll, P., Fiedler, K., and Zhang, J.: Global-scale analysis of river flow alterations due to water withdrawals and reservoirs, Hydrol. Earth Syst. Sci., 13 (12), 2413–2432, doi: 10.5194/hess-13-2413-2009, 2009.

Döll, P., Hasan, H. M. M., Schulze, K., Gerdener, H., Börger, L., Shadkam, S., Ackermann, S., Hosseini-Moghari, S.M., Müller Schmied, H., Güntner, A., and Kusche, J.: Leveraging multi-variable observations to reduce and quantify the output uncertainty of a global hydrological model: evaluation of three ensemble-based approaches for the Mississippi River basin, Hydrol. Earth Syst. Sci., 28 (10), 2259–2295, doi: 10.5194/hess-28-2259-2024, 2024.

Döll, P., Kaspar, F., and Lehner, B.: A global hydrological model for deriving water availability indicators: model tuning and validation, J. Hydrol., 270 (1-2), 105–134, doi: 10.1016/S0022-1694(02)00283-4, 2003.

Dong, N., Wei, J., Yang, M., Yan, D., Yang, C., Gao, H., Arnault, J., Laux, P., Zhang, X., Liu, Y., and Niu, J.: Model Estimates of China's Terrestrial Water Storage Variation Due To Reservoir Operation, Water Resour. Res., 58 (6), e2021WR031787, doi: 10.1029/2021WR031787, 2022.

Dong, N., Yang, M., Wei, J., Arnault, J., Laux, P., Xu, S., Wang, H., Yu, Z., and Kunstmann, H.: Toward Improved Parameterizations of Reservoir Operation in Ungauged Basins: A Synergistic Framework Coupling Satellite Remote Sensing, Hydrologic Modeling, and Conceptual Operation Algorithms, Water Resour. Res., 59 (3), e2022WR033026, doi: 10.1029/2022WR033026, 2023.

Ehsani, N., Fekete, B. M., Vörösmarty, C. J., and Tessler, Z. D.: A neural network based general reservoir operation algorithm. Stochastic environmental research and risk assessment, 30, 1151-1166, doi: 10.1007/s00477-015-1147-9, 2016.

Gutenson, J. L., Tavakoly, A. A., Wahl, M. D., and Follum, M. L.: Comparison of generalized non-data-driven lake and reservoir routing models for global-scale hydrologic forecasting of reservoir outflow at diurnal time steps, Hydrol. Earth Syst. Sci., 24 (5), 2711–2729, doi: 10.5194/hess-24-2711-2020, 2020.

Haddeland, I., Skaugen, T., and Lettenmaier, D. P.: Anthropogenic impacts on continental surface water fluxes. Geophys. Res. Lett., 33(8), doi: 10.1029/2006GL026047, 2006.

Hanasaki, N., Kanae, S., and Oki, T.: A reservoir operation algorithm for global river routing models, J. Hydrol., 327 (1-2), 22–41, doi: 10.1016/j.jhydrol.2005.11.011, 2006.

Hanasaki, N., Kanae, S., Oki, T., Masuda, K., Motoya, K., Shirakawa, N., Shen, Y., and Tanaka, K.: An integrated model for the assessment of global water resources – Part 2: Applications and assessments, Hydrol. Earth Syst., Sci. 12 (4), 1027–1037, doi: 10.5194/hess-12-1027-2008, 2008.

Hanazaki, R., Yamazaki, D., and Yoshimura, K.: Development of a reservoir flood control scheme for global flood models. J. Adv. Model. Earth Sy., 14(3), e2021MS002944, doi: 10.1029/2021MS002944, 2025

Hasan, H. M. M., Döll, P., Hosseini-Moghari, S. M., Papa, F., and Güntner, A.: The benefits and trade-offs of multi-variable calibration of the WaterGAP global hydrological model (WGHM) in the Ganges and Brahmaputra basins, Hydrol. Earth Syst. Sci., 29(2), 567-596, doi: 10.5194/hess-29-567-2025, 2025.

Hosseini-Moghari, S. M., Araghinejad, S., Tourian, M. J., Ebrahimi, K., and Döll, P.: Quantifying the impacts of human water use and climate variations on recent drying of Lake Urmia basin: the value of different sets of spaceborne and in situ data for calibrating a global hydrological model, Hydrol. Earth Syst. Sci. 24 (4), 1939–1956, doi: 10.5194/hess-24-1939-2020, 2020.

Hou, J., Van Dijk, A. I., Renzullo, L. J., and Larraondo, P. R. (2024). GloLakes: water storage dynamics for 27 000 lakes globally from 1984 to present derived from satellite altimetry and optical imaging. Earth Syst. Sci. Data, 16(1), 201-218, doi: 10.5194/essd-16-201-2024, 2024.

Jager, H. I. and Smith, B. T.: Sustainable reservoir operation: Can we generate hydropower and preserve ecosystem values?, River Res. Appl., 24(3), 340-352, doi: 10.1002/rra.1069, 2008.

Kling, H., Fuchs, M., and Paulin, M.: Runoff conditions in the upper Danube basin under an ensemble of climate change scenarios, J. Hydrol., 424, 264-277, doi: 10.1016/j.jhydrol.2012.01.011, 2012.

Knoben, W. J. M., Freer, J. E., and Woods, R. A.: Technical note: Inherent benchmark or not? Comparing Nash–Sutcliffe and Kling–Gupta efficiency scores, Hydrol. Earth Syst. Sci. 23 (10), 4323–4331. doi: 10.5194/hess-23-4323-2019, 2019.

Lamontagne, J. R., Barber, C. A., and Vogel, R. M.: Improved estimators of model performance efficiency for skewed hydrologic data, Water Resour. Res., 56(9), e2020WR027101, doi: 10.1029/2020WR027101, 2020.

Lehner, B., Liermann, C.R., Revenga, C., Vörösmarty, C., Fekete, B., Crouzet, P., Döll, P., Endejan, M., Frenken, K., Magome, J., and Nilsson, C.: High-resolution mapping of the world's reservoirs and dams for sustainable river-flow management, Frontiers in Ecol & Environ 9 (9), 494–502, doi: 10.1890/100125, 2011.

Li, Y., Zhao, G., Allen, G.H., and Gao, H.: Diminishing storage returns of reservoir construction, Nat. Commun., 14(1), 3203, doi: 10.1038/s41467-023-38843-5, 2023.

Masaki, Y., Hanasaki, N., Takahashi, K., and Hijioka, Y.: Consequences of implementing a reservoir operation algorithm in a global hydrological model under multiple meteorological forcing, Hydrolog. Sci. J. 63 (7), 1047–1061, doi: 10.1080/02626667.2018.1473872, 2018.

Müller Schmied, H., Cáceres, D., Eisner, S., Flörke, M., Herbert, C., Niemann, C., Peiris, T.A., Popat, E., Portmann, F.T., Reinecke, R., and Schumacher, M.: The global water resources and use model WaterGAP v2.2d: model description and evaluation, Geosci. Model Dev. 14 (2), 1037–1079, doi: 10.5194/gmd-14-1037-2021, 2021.

Müller Schmied, H., Trautmann, T., Ackermann, S., Cáceres, D., Flörke, M., Gerdener, H., Kynast, E., Peiris, T. A., Schiebener, L., Schumacher, M., and Döll, P.: WaterGAP v2.2e, https://doi.org/10.5281/ZENODO.10026943, 2023.

Müller Schmied, H., Trautmann, T., Ackermann, S., Cáceres, D., Flörke, M., Gerdener, H., Kynast, E., Peiris, T. A., Schiebener, L., Schumacher, M., and Döll, P.: The global water resources and use model WaterGAP v2.2e: description and evaluation of modifications and new features, Geosci. Model Dev., 17, 8817–8852, doi: 10.5194/gmd-17-8817-2024, 2024.

NASA Earth Observatory: https://earthobservatory.nasa.gov/images/83716/lake-powell-half-empty, last access: 20 August 2024.

Nazemi, A., and Wheater, H. S.: On inclusion of water resource management in Earth system models – Part 2: Representation of water supply and allocation and opportunities for improved modeling, Hydrol. Earth Syst. Sci. 19 (1), 63–90, doi: 10.5194/hess-19-63-2015, 2015.

Otta, K., Müller Schmied, H., Gosling, S.N., and Hanasaki, N.: Use of satellite remote sensing to validate reservoir operations in global hydrological models: a case study from the CONUS, Hydrol. Earth Syst. Sci. Discuss., doi: 10.5194/hess-2023-215, 2023.

Perera, D., Smakhtin, V., Williams, S., North, T., and Curry, A.: Ageing water storage infrastructure: An emerging global risk. UNU-INWEH Report Series, 11, 25, 2021.

Rougé, C., Reed, P.M., Grogan, D.S., Zuidema, S., Prusevich, A., Glidden, S., Lamontagne, J.R., and Lammers, R.B.: Coordination and control – limits in standard representations of multi-reservoir operations in hydrological modeling. Hydrol. Earth Syst. Sci., 25 (3), 1365–1388, doi: 10.5194/hess-25-1365-2021, 2021.

Sadki, M., Munier, S., Boone, A., and Ricci, S.: Implementation and sensitivity analysis of the Dam-Reservoir OPeration model (DROP v1.0) over Spain, Geosci. Model Dev., 16, 427–448, doi: 10.5194/gmd-16-427-2023, 2023.

Shah, H.L., Zhou, T., Sun, N., Huang, M., and Mishra, V.: Roles of Irrigation and Reservoir Operations in Modulating Terrestrial Water and Energy Budgets in the Indian Subcontinental River Basins, J. Geophys. Res. Atmos. 124 (23), 12915–12936, doi: 10.1029/2019JD031059, 2019.

Shen, Y., Yamazaki, D., Pokhrel, Y., and Zhao, G.: Improving global reservoir parameterizations by incorporating flood storage capacity data and satellite observations, Water Resour. Res., 61(1), e2024WR037620, doi: 10.1029/2024WR037620 2025.

Shin, S., Pokhrel, Y. and Miguez-Macho, G.: High-Resolution Modeling of Reservoir Release and Storage Dynamics at the Continental Scale, Water Resour. Res., 55 (1), 787–810, doi: 10.1029/2018WR023025, 2019.

Steyaert, J. C., and Condon, L. E.: Synthesis of historical reservoir operations from 1980 to 2020 for the evaluation of reservoir representation in large-scale hydrologic models, Hydrol. Earth Syst. Sci., 28 (4), 1071–1088, doi: 10.5194/hess-28-1071-2024, 2024.

Steyaert, J. C., Condon, L. E., Turner, S. W. D., and Voisin, N.: ResOpsUS, a dataset of historical reservoir operations in the contiguous United States, Sci. Data, 9 (1), 34, doi: 10.1038/s41597-022-01134-7, 2022.

Telteu, C.-E., Müller Schmied, H., Thiery, W., Leng, G., Burek, P., Liu, X., Boulange, J. E. S., Andersen, L. S., Grillakis, M., Gosling, S. N., Satoh, Y., Rakovec, O., Stacke, T., Chang, J., Wanders, N., Shah, H. L., Trautmann, T., Mao, G., Hanasaki, N., Koutroulis, A., Pokhrel, Y., Samaniego, L., Wada, Y., Mishra, V., Liu, J., Döll, P., Zhao, F., Gädeke, A., Rabin, S. S., and Herz, F.: Understanding each other's models: an introduction and a standard representation of 16 global water models to support intercomparison, improvement, and communication, Geosci. Model Dev., 14, 3843–3878, doi: 10.5194/gmd-14-3843-2021, 2021.

Tian, W., Liu, X., Wang, K., Bai, P., Liu, C., and Liang, X.: Estimation of global reservoir evaporation losses, J. Hydrol., 607, 1–9, doi: 10.1016/j.jhydrol.2022.127524, 2022.

Tourian, M. J., Elmi, O., Shafaghi, Y., Behnia, S., Saemian, P., Schlesinger, R., and Sneeuw, N.: HydroSat: geometric quantities of the global water cycle from geodetic satellites, Earth Syst. Sci. Data, 14 (5), 2463–2486, doi: 10.5194/essd-14-2463-2022, 2022.

Turner, S. W. D., Steyaert, J. C., Condon, L., and Voisin, N.: Water storage and release policies for all large reservoirs of conterminous United States, J. Hydrol., 603, 126843, doi: 10.1016/j.jhydrol.2021.126843, 2021.

Turner, S. W. D., Xu, W., and Voisin, N.: Inferred inflow forecast horizons guiding reservoir release decisions across the United States. Hydrol. Earth Syst. Sci. 24 (3), 1275–1291, doi: 10.5194/hess-24-1275-2020, 2020.

Vanderkelen, I., Gharari, S., Mizukami, N., Clark, M.P., Lawrence, D.M., Swenson, S., Pokhrel, Y., Hanasaki, N., Van Griensven, A., and Thiery, W.: Evaluating a reservoir parametrization in the vector-based global routing model mizuRoute (v2.0.1) for Earth system model coupling, Geosci. Model Dev. 15 (10), 4163–4192, doi: 10.5194/gmd-15-4163-2022, 2022.

Vora, A., Cai, X., Chen, Y., and Li, D.: Coupling reservoir operation and rainfall-runoff processes for streamflow simulation in watersheds, Water Resour. Res., 60(6), e2023WR035703, doi: 10.1029/2023WR035703, 2024.

Wang, J., Walter, B. A., Yao, F., Song, C., Ding, M., Maroof, A. S., Zhu, J., Fan, C., Xin, A., McAlister, J. M., and Sikder, S.: GeoDAR: georeferenced global dams and reservoirs dataset for bridging attributes and geolocations, Earth Syst. Sci. Data, 14 (4), 1869–1899, doi: 10.5194/essd-14-1869-2022, 2022.

Yassin, F., Razavi, S., Elshamy, M., Davison, B., Sapriza-Azuri, G., and Wheater, H.: Representation and improved parameterization of reservoir operation in hydrological and land-surface models, Hydrol. Earth Syst. Sci. 23 (9), 3735–3764, doi: 10.5194/hess-23-3735-2019, 2019.

Zajac, Z., Revilla-Romero, B., Salamon, P., Burek, P., Hirpa, F. A., and Beck, H.: The impact of lake and reservoir parameterization on global streamflow simulation, J. Hydrol., 548, 552–568, doi: 10.1016/j.jhydrol.2017.03.022, 2017.